Fire Research Note No. 712

THE CONTRIBUTION OF FLAMES UNDER CEILINGS TO FIRE SPREAD IN COMPARTMENTS PART I. INCOMBUSTIBLE CEILINGS

by

P. L. HINKLEY, H. G. H. WRAIGHT and C. R. THEOBALD

FIRE RESEARCH STATION

THE CONTRIBUTION OF FLAMES UNDER CEILINGS TO FIRE SPREAD IN COMPARTMENTS

PART I. INCOMBUSTIBLE CEILINGS

by

P.L. Hinkley, H.G.H. Wraight and C. R. Theobald

SUMMARY

This report describes the detailed measurements in an experimental investigation of flames spreading under an incombustible ceiling. Later reports will deal with combustible ceiling linings and the practical applications of the work.

Experiments were performed in a model representing the ceiling of a corridor with a fire at one end - a gas burner was used to represent the fire, this was replaced by wooden cribs in experiments to be described in a later report.

Depending on the size of the fire and its distance beneath the ceiling, the flames may have drawn up into the horizontal layer of hot gases enough air for combustion of the fuel gases. The flame length is then determined by mixing within the layer. The air drawn up may not be sufficient for the combustion of the gases from large fires and the remaining air required for combustion is entrained vertically into the hot gases flowing over the cooler air beneath.

Correlations of horizontal flame lengths have been derived and related to the much shorter lengths of vertical flames.

Relationships have been derived from the experimental data from which it is possible to estimate the radiation downwards from the hot ceiling and the gases beneath it to the floor with a view to estimating the contribution to fire spread on the floor.

A heat balance of the ceiling gases was satisfactory, so confirming the validity of the calculations. Horizontal flames radiate more of the heat produced at a level sufficient to assist fire spread than do vertical ones.

MINISTRY OF TECHNOLOGY AND FIRE OFFICES' COMMITTEE

ABSTRACT

In order to devise rational tests and performance requirements for flammable linings in various positions in buildings, one must have some quantitative design criteria either from direct experience or from research and, although much experimental work has been done, in the U.K. and overseas, there are still many difficulties in presenting a clear description of the processes of fire growth and the contribution to this of the many factors involved. Thus, it is deceptively easy to devise tests for linings but so far impossible to get an agreed order of merit between various materials subjected to tests ostensibly designed for the same purpose.

In parallel with an experimental international study covering the role of many factors in fire growth, certain fundamental features of fire growth are being studied in detail, and this report is the first one of a series investigating the characteristics of flames beneath various kinds of ceilings. The special feature of fires in enclosed spaces is that at some stage the flames from materials on the floor are deflected by the ceiling and extend horizontally. This, as the report shows, dramatically increases the radiation to unburnt fuel away from the fire, and this alone will lead to fire spread irrespective of other influences, even under incombustible ceilings.

This report is essentially a detailed scientific description of the work. Its practical implications will be dealt with elsewhere.

The most important results of this study are as follows:

There are various different conditions of burning, for example if the fire is close to the ceiling (as from the top of a high stack) the flames are of a type different from those from a lower source. The former are fuel-rich, the latter air-rich, and different laws apply relating the flame length to the rate of burning. For air-rich flames below part of a ceiling between two parallel screens

$$L = 220 \left(\frac{m'}{\rho_o \, g^{\frac{1}{2}}} \right)^{\frac{2}{5}}$$

where m' is flow rate of fuel per unit width of flow path

ρ_o is density, taken as that of air

and g is acceleration due to gravity

L is measured from a virtual origin which is between 4.3 and 5.3 times the depth of the layer of hot gases beneath the ceiling, i.e. between 2.0 and 2.7 times the distance of the floor fire below the ceiling.

These flames are at least five times the length of vertical flames produced by the same burning rate of fuel.

The radiation emitted downwards from an asbestos ceiling heated by the flame was

$$I = 50 \exp (-4.05X/l) \text{ W/cm}^2$$

where X is the distance from the virtual origin of the flames and the heat transfer to the ceiling was

$$H = 70 \exp(-4.6X/l) \text{ W/cm}^2$$

These equations do not apply between the virtual origin of the flames and the actual origin. A maximum rate of heat transfer rate to the ceiling of 17 W/cm^2 has been recorded at the latter position.

Calculations based on the experimental measurements have been made of the relative proportions of the heat output of the flames transferred by radiation from the flames and the ceiling behind them, by conduction through the ceiling and walls and by convection in the hot gas layer. The heat transferred by radiation is up to four times greater from horizontal flames than from vertical ones.

THE CONTRIBUTION OF FLAMES UNDER CEILINGS
TO FIRE SPREAD IN COMPARTMENTS

PART I. INCOMBUSTIBLE CEILINGS

LIST OF SYMBOLS IN ALPHABETICAL ORDER

a = Maximum value of θ "seen" by radiometer disc.

B = Specific heat of hot gases.

C_p = Specific heat of gases in layer.

c = Molecular diffusion coefficient.

D = Shorter dimension of fuel bed.

D_p = Diameter of pitot head.

d = Depth of layer of hot gases.

d_c = Thickness of asbestos wood.

d_f = Layer depth at virtual origin.

d_s = Depth of end screen.

g = Gravitational acceleration.

H = Heat transfer to ceiling.

H_c = Heat loss through ceiling.

H_g = Convective heat transfer coefficient for underside of ceiling.

H_o = Heat transfer to ceiling at virtual origin.

H_u = Convective heat transfer coefficient from topside of ceiling.

h = Depth of burner below ceiling.

I = Radiation intensity from base of hot gas layer.

I_c = Radiation intensity immediately above radiometer.

I_g = Radiation intensity on ceiling

I_o = Radiation intensity at virtual origin.

I_r = Radiation intensity recorded by radiometers.

I_v = Radiation intensity from vertical flames.

K = Constant.

K_c = Thermal conductivity of asbestos wood.

k, k' = Constant.

L = Flame height.

L_t = Flame height measured to tip.

l = Flame length measured from virtual origin.

M = Total mass flow rate of hot gases.

M_f = Mass flow rate of town gas from burner.

M_v = Mass rate of entrainment.

M'' = Mass flow rate of hot gases per unit area.

$(M_v)_1$ = Momentum flow beneath ceiling.

$(M_v)_2$ = Momentum flow of hot gases entering layer.

m' = Flow rate of town gas from burner per cm width.

m'' = Burning rate per unit area of fuel bed.

Q_f = Rate of heat gain by combustion.

Q_l = Convective heat transfer with flow of hot gases.

Q_r = Rate of heat loss by radiation.

Q_u = Rate of heat loss through ceiling and screens.

T = Absolute temperature of hot gases.

T_c = Absolute temperature of underside of ceiling.

T_o = Absolute temperature of ambient air.

T_u = Absolute temperature of topside of ceiling.

u = Upward velocity of entrained air.

u_1 = Velocity of luminous flames.

u_2 = Speed of travel of film in camera.

V = Volume flow rate of air and fuel gas.

V_f = Volume flow rate of town gas.

v = Velocity of layer of hot gases.

w = Width of corridor.

X = Horizontal distances measured from virtual origin $(x + x_o)$.

x = Horizontal distance measured from rear of corridor.

x_o = Distance of virtual origin behind rear of corridor.

y = Height above bottom of layer.

z = "Dummy" variable.

Z = Pitot tube anemometer reading in cm. water gauge.

α = Angle of track on film with film margin.

β = Magnification of camera optical system.

ε = Emissivity.

θ = Temperature excess over ambient.

Δ = Increase in heat carried as latent heat of water vapour.

ν = Kinematic viscosity.

ξ = Horizontal distance from point immediately over radiometer.

ρ = Density.

ρ_g = Density of town gas.

ρ_o = Density of gas in layer reduced to N.T.P.

ρ_w = Density of water.

σ = Stefan's constant.

ϕ = Configuration factor.

ϕ_a = Configuration factor at radiometer of bottom of hot gas layer.

THE CONTRIBUTION OF FLAMES UNDER CEILINGS TO FIRE SPREAD IN COMPARTMENTS

PART I. INCOMBUSTIBLE CEILINGS

by

P. L. Hinkley, H.G.H. Wraight and C. R. Theobald

1. INTRODUCTION

The "flashover" of a fire in a compartment is generally defined as the stage when fire quickly spreads to involve the entire compartment[1]. The time taken for flashover to occur is of practical importance in determining the possibility of escape by the occupants and the size of the fire on the arrival of the fire brigade. In the past many experiments have been undertaken to study the growth of the fire to flashover and the way in which this is affected by the geometry of the compartment and the materials of which it is composed.[1]

A method frequently adopted has been to construct a compartment (either full size or a model) and to carry out experiments with an arrangement of combustible contents over which fire is found to spread in a repeatable way and at a convenient rate. The influence of changing various features (often the wall and ceiling linings) is then studied.

While such an approach has yielded much useful information it has so far thrown little light on the physical and combustion processes occurring in the important transition between the fire behaving as it would in the open and "flashover".

When the fire on the ground has grown to the extent that flames have reached the ceiling, any further increase in size must result in flames extending horizontally beneath the ceiling; this configuration is expected to result in a greatly increased rate of heat transfer, back to the floor as well as to the ceiling itself. At the same time it is expected that the rate of entrainment of air will be much less than for vertical ones. Clearly, it is to be expected that this horizontal spread of flame with its influence on the thermal feedback to the floor must play a vital role in the growth of fire.

Little information could be found about flames of this type and experiments were therefore directed towards determining their characteristics and in particular the rate of transfer of heat from them both to the ceiling and the floor beneath.

Experiments were carried out in models representing a corridor with a fire at one end. A corridor was chosen because the flow of gases along a corridor in one direction should be simpler to study than radial flow beneath a flat ceiling both from the theoretical and the experimental stand-point. This configuration is directly applicable not only to spread in corridors but also to spread along the bays of buildings with sawtooth and similar roofs; the flow in many other situations is frequently more uni-directional than radial.

The models each comprised a long ceiling with screens hanging down from its edges to channel the hot gases along it, but were effectively without floors. They were mounted sufficiently far above the floor of the laboratory to present no hindrance to the entrainment of air by the flames and to prevent the floor becoming hot enough to significantly affect the heat balance. This was done firstly for safety, there was no opportunity for the formation of pockets of an explosive mixture; secondly, it enabled the horizontal flames to be studied in isolation without the complicating factor of the "feedback" of heat from the floor and finally it greatly simplified instrumentation and observation of the flames.

The effect of a floor to a model corridor will be reported in a later note.

The fuel used was town gas because it was an easily available fuel of known calorific value and the rate of input of fuel could be easily set to a known value which did not depend on the rate of feedback of heat to the fuel. This enabled effects of the horizontal flames, due to the heating up of the ceiling and walls, to be separated from those due to the increase in burning rate of the fuel. However, town gas is a mixture of gases which differs from that produced by the pyrolysis of cellulosic materials, which are those most frequently involved in fires and the differences in heat transfer rates due to this factor will be discussed in another note.

2. EXPERIMENTAL CORRIDORS

The town gas burner incorporated in the experimental apparatus was based on one described elsewhere[2], and consisted essentially of a tray of exfoliated vermiculite having a horizontal surface area of 46 x 115 cm through which the town gas percolated. The distance of the surface of the burner beneath the ceiling could be varied from 37 to 120 cm.

The ceiling of the model corridor used in most of these experiments (Fig. 1 Plate 1) was 7.3 metres long and 1.2 metres wide and was mounted 1.8 metres above the concrete floor of the laboratory, with its rear end over the burner. It was made of 1.27 cm thick asbestos wood and was fitted with screens along the sides and at the rear end to channel the hot gases from a fire. The screen at the

rear and the first 1.2 metres of the side screens were made of 1.27 cm thick asbestos wood and the remainder of the side screens were made of 0.48 cm thick asbestos millboard. The screens varied in depth from 120 cm at the closed end to 50 cm at the open end (Fig. 1).

In a few early experiments a corridor 80 cm wide and 5.8 metres long was used. This was basically similar to the one described above but the burner was 51 cm x 63.5 cm in area and was fixed 37 cm beneath the ceiling. In addition the open end of the corridor could be partly closed by an asbestos wood screen extending downwards from the ceiling.

3. EXPERIMENTAL MEASUREMENTS

The positions of the measuring devices in the corridor during the main experiments are shown on Fig. 1.

3.1. Radiation

The intensity of radiation downwards from the layer of flame and hot gases was measured by a line of six radiometers[3,4], facing upwards along the centre line of the corridor and generally 66 cm beneath the ceiling; in this position the contribution of the radiation from the portion of the screens below the level of the layer of hot gases to the measured intensity was negligible since the acceptance angle of the radiometers was effectively only 135 degrees. In experiments with the burner 37 cm beneath the ceiling the radiometers were also 37 cm beneath the ceiling. The intensity of radiation immediately in front of the burner was too high to be measured by the available radiometers, and a total radiation pyrometer with an arsenic tri-sulphide lens was therefore directed upwards at the ceiling at this point. The radiation from the vertical flames was measured by a narrow angle total radiation pyrometer with a similar lens directed along the corridor.

3.2. Ceiling temperatures

Ceiling temperatures were measured by twelve chromel-alumel thermocouples along the centre line of its lower surface. The couples were attached by silicate paint in grooves so that they were flush with the lower surface of the ceiling.

3.3. Heat transfer to ceiling

The rates of heat transfer to the ceiling were calculated from the equilibrium ceiling temperatures as described in Appendix 1. It was found difficult to ensure good contact between the ceiling and the thermocouple immediately over the burner, and the rate of heat transfer to the ceiling at this point was measured by a water flow calorimeter[5].

3.4. Temperature of hot gas stream

The vertical temperature distribution within the layer of hot gases flowing beneath the corridor ceiling at 2.0 and 5.2 metres from the end screen was measured by two 40 S.W.G. thermocouples which could be moved vertically within the layer.

Owing to radiation losses, the thermocouple attained a temperature below the actual temperature of the hot gas layer. The magnitude of the error depended on the intensity of radiation falling on the thermocouple and the temperature and velocity of the stream of hot gases. It was probably of the order of 100 deg C when the thermocouple was reading 600°C near the ceiling and 200 deg C when the thermocouple was reading 800°C near the bottom of the layer.*

3.5. Velocity of horizontal luminous flames

The velocity of the horizontal luminous flames was measured using a "streak" camera (Fig. 2). This was a continuous film oscillograph recording camera modified by fixing, immediately in front of the film, a diaphragm with a 1.5 mm wide slit perpendicular to the direction of motion of the film. A stainless steel mirror was mounted beneath the ceiling so as to reflect an image of the flames through a right angle into the camera which was mounted on its side with the axis of the slit parallel to the ceiling. The camera and mirror were enclosed in a box covered with aluminium on the outside and painted black on the inside; an aperture above the mirror permitted light from the flames to enter the camera after reflection in the mirror.

A typical streak photograph (Plate 2) showed the variation in the appearance of a 2 cm wide x 80 cm long strip along the axis of the ceiling with time, the time axis runs from right to left along the photograph.

---

*These estimates were derived from measured intensities of radiation as described by Heselden.[2]

The photographs showed luminous flames moving steadily down the corridor; the slope of their tracks in the photograph was related to the velocity beneath the corridor ceiling

$$u_1 = (u_2/\beta) \tan \alpha$$

where u_1 was the velocity of the luminous flames

u_2 was the speed of travel of film in camera

$\tan \alpha$ was the mean slope of the tracks on the photographic film

and β was the magnification. This was determined by photographing a number of lamps attached at measured intervals along the ceiling.

3.6. Velocity of hot gases

In three experiments the vertical distribution of velocity at 2.0 and 5.2 metres from the rear screen was measured by a water cooled pitot static tube in conjunction with a diaphragm capacitance differential micro-manometer having a full scale deflection of either 0.1 or 1.0 mm w.g. The measuring head of the pitot tube was inclined at an angle of about 3° to the horizontal with the tip upwards to prevent condensation collecting round the holes.

3.7. Oxygen content of hot gas layer

In some preliminary experiments the gases in the layer beneath the ceiling were sampled through a water-cooled probe with its inlet pointing upstream, filtered through glass wool to remove solids and dried by silica gel. The oxygen content of the dry gases was measured using a Beckmann paramagnetic oxygen analyser.

3.8. Data recording and processing

In the earlier experiments the instruments were connected to twelve-way automatic switching units and were switched for three seconds at a time to D.C. amplifiers; the outputswere recorded by pen recorders. In the later experiments all the instruments (except the 40 S.W.G. probe thermocouples, the narrow angle pyrometer and the water flow calorimeter) were connected to an electronic data logging system. This took spot readings of each of the instruments in turn, measured their output with a digital voltmeter and recorded them on punched tape with an accuracy of about $\pm$ 0.05 mV. Readings were taken once every minute until equilibrium had been reached (usually about 20-25 minutes) when a further twelve readings were taken at half minute intervals.

The punched tapes were subsequently processed by a computer to convert the outputs of the digital voltmeter to temperatures or heat transfer rates which were then tabulated. The means of the readings taken after the attainment of equilibrium were also tabulated.

3.9. Instrumentation in preliminary experiments

In the preliminary experiments measurements were made at a position approximately halfway along the corridor of vertical temperature distribution, ceiling temperature, radiation downwards, luminous flame velocity, and (in a few experiments) oxygen content of the hot gases. The instruments used were similar to those described above.

4. EXPERIMENTS PERFORMED

Preliminary experiments in the smaller corridor with limited instrumentation were carried out at four main rates of flow of town gas (125, 212, 250 and 375 cm^3/s per cm width of corridor) and with three depths of screen at the front end of the corridor (0, 15 and 23 cm). A few experiments were carried out at other rates of town gas flow.

The main experimental programme with the larger corridor comprised experiments at five town gas flow rates (300, 250, 183, 125 and 83 cm^3/s per cm width of corridor) at each of four distances beneath the ceiling (37, 66, 90 and 120 cm). There was no screen at the front end in any of these experiments.

5. EXPERIMENTAL RESULTS AND DISCUSSION

There were no significant differences between the results of the preliminary experiments and those of corresponding experiments in the main programme. The results of the preliminary experiments have therefore been included with the results of the main programme where appropriate.

5.1. Appearance of flames

Except when the gas burner was at its highest position (37 cm beneath the ceiling) the flames travelling horizontally beneath the ceiling had the appearance of horizontal extensions of the ones rising vertically from the burner although the horizontal flames were much longer than the vertical ones would have been. At high rates of gas flow the flames beneath the ceiling near the burner appeared to be continuous and to extend throughout the depth of the layer of hot gases but further away they disintegrated into "balls" which travelled for some distance along the corridor. At lower rates of flow of town gas only balls of flame travelled beneath the ceiling. Beyond the point where the balls ceased to be luminous

they could sometimes be seen to continue travelling along the corridor as smoke vortices; this was particularly noticeable when the burner was 120 cm beneath the ceiling.

When the burner was 37 cm beneath the ceiling the flames had an appearance similar to that described above at low rates of flow of town gas. However, at higher rates of flow of town gas (above about 150 cm^3/s per cm width of burner) the layer appeared to be starved of oxygen and the flames had the appearance shown in Plate 3 and diagrammatically in Fig. 3. Near the burner they were generally confined to the bottom of the layer of hot gases but tongues of flame reached upwards into the layer. Away from the burner the upward-reaching tongues of flame increased in length until they licked the ceiling. Further away from the burner the horizontal flames broke into separate pockets which travelled inside the layer for one or two metres.

The upward tongues of flame appeared thicker than the remainder of the flames when viewed from beneath and therefore appeared as the bright patches in the streak photographs. The general circulation of the gases within the layer along the centre of the corridor is indicated in Fig. 3a; at the sides of the corridor the circulation was modified by the cooling effect of the walls and the flow was downwards at the walls as shown in Fig. 3b.

5.2. Air-rich and fuel-rich layers

The visual observation of the flames suggested the existence of two regimes of burning; one in which sufficient air to burn the town gas was entrained by the vertical portions of the flames and subsequent combustion was controlled by mixing within the layer of hot gases, and the other in which the layer contained insufficient air to burn all the town gas and combustion was controlled by the limited entrainment of air into the bottom of the layer.

The results of the experimental measurements described later in this report are in accord with this interpretation of the visual observations and, although the border between the two regimes was not well defined, these situations in which the heat transfer rates and other parameters have been modified by lack of oxygen within the layer will be described as lying within the fuel-rich regime and the other situations as lying within the air-rich regime.

5.3. Flame length measurements

Measurements of the length of vertical flames[6] have usually been made to the mean position of the oscillating tips, ignoring detached portions. However, this measurement was found to be difficult to make with the horizontal flames and visual estimates were therefore made of the distances to which the balls of flame travelled; these (for the main series) are given in Table 1.

Table 1

Lengths of horizontal flames

(measured to tips)

Distance of burner beneath ceiling cm	Town gas flow cm^3/s per cm width of corridor				
	300	250	183	125	83
	Flame tip length - m				
120	5.0	4.0	2.5	1.5	0.0
90	6.5	4.5	4.0	3.0	1.0
66	7.3 6.5	5.0 4.5	3.6 3.5	2.0	1.5 0.5
37	7.3+	7.3+	-	3.0	1.3

5.4. Vertical temperature and oxygen profiles

The ways in which the vertical distribution of temperature within the layer of hot gases measured by 40 S.W.G. thermocouples varied with gas flow, distance of burner beneath the ceiling and distance from the rear of the corridor are shown in Figs. 4-6. The relation between the shapes of the temperature profiles and the oxygen concentration profiles within the layer is shown in Figs. 7-9 which give measurements made at about 2.2 metres from the rear of the smaller corridor with the burner 37 cm beneath the ceiling. In the air-rich regime combustion occurred close to the ceiling (Fig. 7) but as the air/town gas ratio decreased the combustion zone became thicker with the maximum temperature occurring nearer the bottom of the layer (Fig. 8) while in the fuel-rich regime combustion occurred at the bottom of the layer (Fig. 9) with a consequent peak in the temperature profile at that point.

5.5. Depth of hot gas layer

The position of the bottom of the layer of hot gases was found from the measured temperature distributions. Owing to the effects of radiation, the reading of the thermocouple was not zero beneath the layer and the bottom was defined by extrapolating the steep portion of the curve within the layer and the shallow portion outside to meet at a point (Fig. 10). In a number of experiments, the bottom of the layer was outside the range of travel of the probe thermocouple and could only be found approximately by extrapolation. The depths of the layer of hot gases during the main experiments are given in Table 2. The depth of the layer of hot gases did not vary with the rate of flow of town gas except when the burner was 37 cm beneath the ceiling; when the rate of entrainment of air by the vertical flames was low enough to be comparable with the rate of flow of town gas. The depth of the layer of hot gases when the burner was 37 cm beneath the ceiling, is shown in Fig. 11.

The layer of hot gases was generally thicker at 2.0 metres from the rear of the corridor than at 5.2 metres; there was no difference when the burner was 37 cm beneath the ceiling.

The layer of hot gases thickened as the distance of the burner beneath the ceiling increased. When the layer was air-rich and there was no screen at the front end of the model, the depth of the layer of hot gases was nearly half the distance of the burner beneath the ceiling (Fig. 12), this linear relationship did not hold at 5.2 metres from the rear of the corridor.

5.6. Velocities of luminous flames

The velocities of the luminous flames measured using the "streak" camera are given in Table 3. These velocities correspond to the velocities of the hot gases in the plane of the flames i.e. near the ceiling when the layer was air-rich and near the base of the layer when it was fuel-rich.

In the air-rich regime the velocity was almost proportional to $d^{\frac{1}{2}}$, where d was the depth of the layer of hot gases (Fig. 13).

Table 2

Depths of layer of hot gases

Distance of burner beneath ceiling cm	Town gas flow per cm width of corridor cm^3/s	Distance from rear m	
		2.0	5.2
		Depth of layer cm	
37	300	26	26
	250	24	25
	183	22	23
	125	19	19
	83	18	18
66	300	32	27
	250	-	31
	183	30	29
	125	31	29
	83	-	-
90	300	40-50*	36
	250		36
	183		38
	125		36
	83		38
120	300	50-60*	
	250		
	183		40-50*
	125		
	83		

*Based on extrapolation of temperature distribution

Table 3

Velocity of luminous flames

Distance of burner beneath ceiling cm	Town gas flow cm^3/s per cm width of corridor	Distance from rear m			
		0.8	2.0	3.5	5.2
		Velocity m/s			
120	183	4.11			
	250	4.38	3.55		
	300	4.52	4.81		
90	183	4.22	3.34		
	250	4.35	3.51		
	300	3.78	3.38		
66	183		2.86		
	250		2.87		
	300		2.73	2.88	
37	125	2.16	2.07		
	183		2.08	1.82	
	212		1.08		
	250		1.03	1.49	
	300		0.98		1.66
	375		0.68		

5.7. Pitot tube measurements

Measurements were made of the vertical velocity profile at 2.0 and 5.2 metres from the rear when the burner was 66 cm beneath the ceiling.

The micromanometer used with the pitot tube expressed the pressure difference in terms of centimetres of water and the velocity of the layer of hot gases was calculated using the equation

$$v = (2g Z \rho_w T/\rho_o T_o)^{\frac{1}{2}}$$

where Z was the anemometer reading (centimetres of water)

ρ_w was the density of water

ρ_o was the density of the gases in the layer at N.T.P. (this was assumed to be approximately equal to the density of air).

T was the absolute temperature of the hot gases

T_o was the absolute ambient temperature.

Measurements of the velocity distribution are shown in Fig. 14. The accuracy of a pitot tube at low velocities depends on the temperature of the gases since it is a function of the Reynolds number vD_p/ν

where D_p was the diameter of the pitot head

and ν was the kinematic viscosity of the hot gases (which increases with temperature).

In the worst instances the Reynolds number corresponding to velocity measurements 2.0 metres from the rear of the corridor was only about 400 at the intermediate rate of flow of town gas and 250 at the highest rate of flow of town gas, but in these two instances the velocities measured by the pitot tube at the height where the luminous flames occurred agreed with the velocities of the luminous flames measured by the streak camera. This confirms that the pitot tube data were meaningful even in the doubtful instances. Generally the Reynolds numbers were about 500.

The accuracy of the pitot tube becomes uncertain at velocities corresponding to Reynolds numbers of the flow round the pitot head of less than about 500.

The main errors may have been those associated with the difficulties of measuring the small pressures involved.

5.8. Mass flow rate of hot gases

The mass flow rate of hot gases across unit area perpendicular to the flow was calculated from

$$M'' = v\rho = (2g\, Z\, \rho_w \rho_o\, T_o/T)^2$$

The total mass rate of flow of hot gases per cm width of model was obtained by graphical integration and the results are given in Table 4.

Table 4

Flow of hot gases (burner 66 cm beneath ceiling)

Town gas flow rate per cm width		Distance from rear	Peak velocity	Momentum flow per cm width	Mass flow per cm width	Heat flow per cm width	Air flow / Gas flow
cm^3/s	g/s	m	m/s	g cm s^{-2}	g/s	W	
83	0.048	2.0	1.8	300	2.5	840	51
		5.2	1.6	340	-	800	
183	0.106	2.0	2.8	490	2.5	1,600	23
		5.2	2.0	610	-	1,000	
300	0.173	2.0	2.8	540	2.5	2,000	13
		5.2	2.5	790	3.3	1,450	18

At the low rates of town gas flow the position of the bottom of the layer 5.2 metres from the rear of the model was not sufficiently clear to enable M'' to be obtained.

The mass flow per cm width of model 2.0 metres from the rear was 2.5 g/s at all rates of town gas flow. It was much greater than the minimum necessary for complete combustion of the town gas.

At a town gas flow rate of 300 cm^3/s per cm width the mass flow rate of hot gases increased by 0.8 g/s per cm width between 2.0 and 5.2 metres from the rear; this was equivalent to an upward velocity of entrained air (u) of about 1.9 cm/s and an "entrainment constant" u/v of about 0.008 compared with about 0.1 for vertical flames.

The mass rate of entrainment of air by the vertical portion of the flames was given by a simple theory based on experiments[8] as

$$M_v = 0.096\, w \rho_o\, (h-d)^{3/2}\, (g\, T_o/T)^{\frac{1}{2}}$$

Putting the ratio $T_o/T = 0.25$, $\rho_o = 1.3 \times 10^{-3}$ g/cm^3, w = 1.0 cm and (h-d) = 36 cm we obtain

$$M_v = 0.4 \text{ g/s per cm width of corridor.}$$

The total mass flow rate of hot gases is given by

$$M = M_v + M_f$$

where M_f is the mass flow rate of town gas from the burner.

A town gas flow rate of 300 cm/s per cm width is equivalent to about 0.2 g/s per cm width i.e. M ≃ 0.6 g/s per cm width.

If the rate of entrainment of air by the horizontal flames between the burner and the plane at 2.0 metres from the rear of the corridor was the same as that between 2.0 and 5.2 metres from the rear, the mass entrained between the burner and the 2.0 metre plane was about 0.4 g/s. Thus the calculated flow of hot gases at 2.0 metres from the rear was about 1.0 g/s per cm width which must be compared with the measured flow of 2.5 g/s (which was independent of town gas flow rate). The unexpectedly large entrainment may have occurred into the horizontal flames near the burner (because of increased turbulence caused by the change in direction of the hot gases) or it may have occurred into the vertical flames above the burner due to their confinement by the rear and side screens.[8]

5.9. Entrainment into fuel-rich layer

When flames occurred at the bottom of the layer of hot gases the heating of the lower parts of the layer resulted in convection currents within the layer.

The increased vertical mixing made it likely that the velocity of the flames measured by the streak camera was the same as the velocity of the gases over most of the depth of the layer.

In the instances where velocity measurements were made at two distances from the rear of the corridor with the burner 37 cm beneath the ceiling, the rate of entrainment of air between the two measuring points was calculated and the results given in Table 5.

Table 5

Entrainment into fuel-rich layer

Town gas flow rate cm^3/s per cm width of corridor	Distances at which measurements were made m	Upward velocity of entrained air cm/s	Entrainment constant
250	2.0 - 3.5	1.9	0.015
300	2.0 - 5.2	1.7	0.013

The upward velocity of the entrained air is the same as that calculated for the air-rich regime but because the measured velocity of the layer was rather less the entrainment constant is apparently higher.

5.10. Momentum of hot gas layer

The rate of transfer of momentum across a unit area perpendicular to the flow was given by

$$M'' v = v^2 \rho = 2 g Z \rho_w$$

where M'' was the mass rate of flow per unit area.

The pitot tube measured momentum directly and its calculation did not involve a knowledge of the temperature of the layer of hot gases. The rate of transfer of momentum across a vertical strip of unit width perpendicular to the flow, (obtained by graphical integration) is given in Table 4. The momentum at 5.2 metres from the end screen was greater than that at 2.0 metres particularly at high rates of flow of town gas.

This change in momentum was of the same order as the difference between the buoyancy forces acting in the two positions which was given by the difference between the integrals (evaluated graphically)

$$\rho_o g \int_o^d dy \int_o^y \frac{\theta}{T} dz = \rho_o g \int_o^d (d-z) \frac{\theta}{T} dz$$

where y was the height above the bottom of the layer in the two positions, and z is a "dummy" variable.

The momentum of the horizontal flow could have been derived partly from the flow of hot gases out of the end of the corridor and partly from pressure differences caused by the effect of the ceiling on the momentum of the hot gases rising from the fire. Treating the flow out of the end of the corridor as flow over a weir the momentum flow out of the end of the corridor may be shown to be given by

$$(M_v)_1 = 0.54 wg \rho_o d^2 \theta/T$$

In the experiments d was about 30 cm, at the lowest rate of flow of town gas $\theta \simeq 300^{\circ}C$ so that $(M_v)_1 \simeq 300$ g cm s^{-2} per cm width. This is of the same order as that measured at 5.2 metres from the rear of the corridor (340 g cm s^{-2}).

At the highest rate of flow of town gas $\vartheta \simeq 600^{\circ}C$ and $(M_v)_1 \simeq$ 400 g cm s^{-2} per cm width which was about half of that measured 5.2 metres from the rear (790 g cm s^{-2}).

The upward velocity of the flames entering the bottom of the hot layer was estimated[8] to be 0.9 $g^{\frac{1}{2}}$ $(h-d)^{\frac{1}{2}}$ which was about 2.0 m/s so that by using measurements at 2.0 metres from the rear screen and assuming that the rate of entrainment into the horizontal layer was independent of position, the mass flow rate of hot gases entering the layer was estimated to be about 2.0 g/s. The momentum flow of the hot gases entering the layer was $(M_v)_2 \simeq$ 400 g cm s^{-2} per cm width.

Thus at the highest rate of flow of town gas the measured rate of transfer of momentum across a plane perpendicular to the flow 5.2 metres from the rear of the corridor could be accounted for by assuming that pressures due to the destruction of momentum in the hot gases rising vertically from the fire imparted some horizontal momentum to the gases in the layer beneath the ceiling.

5.11. Rate of convective heat flow

The convective heat transfer across unit area perpendicular to the flow of hot gases was given by

$$\dot{Q}_1 = M C_p \vartheta$$

where C_p is the specific heat of the gases

and ϑ was their temperature above ambient

The rate of convective heat transfer per unit width of corridor (obtained by graphical integration) is also given in Table 4. These results will be discussed later.

5.12. Radiation from vertical flames

The intensities of radiation measured by the pyrometer directed at the vertical parts of the flames increased with the town gas flow but decreased as the distance of the burner beneath the ceiling increased.

5.13. Radiation downwards

The radiometers had an acceptance angle[4] of about 135° and being 66 cm beneath the ceiling they accepted little radiation from the sides of the corridor below the level of the bottom of the layer of hot gases. The effective configuation factor of the bottom of the layer of hot gases varied from about 0.75, when the layer was 18 cm deep, to 0.85 when it was more than 40 cm deep. Thus any uncertainty of the effective position of the bottom of the layer of hot gases did not greatly affect the configuration factor.

It is shown in Appendix 2 that the intensity of radiation from the base of the layer of hot gases at a point immediately over a radiometer was given by

$$I_o \simeq I_r/\emptyset$$

where I_r was the intensity recorded by the radiometer
and $\emptyset$ was the configuration factor.
Some typical intensities of radiation at the bottom of the layer of hot gases are shown on Figs. 15a and b.

Values of flame lengths were obtained visually and also by defining the flame tips as the point where the radiation intensity had dropped to 0.9 W/cm^2. Fig. 16 shows that the two methods are in fair agreement.

The intensity decreased roughly exponentially with distance along the corridor when the layer was air-rich and the intensity exceeded about 1.0 W/cm^2. When the layer was fuel-rich the rate of decrease of intensity was less than when it was air-rich (Fig. 15a).

It was found graphically (Fig. 17) that in the air-rich regime the exponential portions of the intensity-distance curves had the equation

$$I/I_o = \exp \left[-k\ (x_o + x)/l\right] = \exp k\ X/l$$

where x was distance measured from the rear of the corridor.
X was the distance measured from a "virtual origin."
x_o was the distance of the virtual origin behind the rear of the corridor. This was between 2.0 and 2.7 times the distance of the burner beneath the ceiling but was apparently independent of the rate of flow of town gas (Table 6).
k was a constant having the value 4.0
l was the flame length measured from the virtual origin (the flame tips were defined as the point where I = 0.9 W/cm^2 (Table 7)).
and I_o was the effective intensity of radiation at the virtual origin and had the value 50 W/cm^2.

Table 6

Distance of virtual origin of horizontal flames behind rear of corridor

Distance of burner beneath ceiling cm	Distance of virtual origin behind rear of corridor (x_o) cm	Ratio of x_o to distance of burner beneath ceiling
37	100	2.7
66	140	2.1
90	180	2.0
120	240	2.0

Table 7

Flame lengths (measured from virtual origin)

Rate of flow of town gas per cm width cm^3/s	Flame length cm
300	700
250	620
183	500
125	390
83	270

The interpretation of Fig. 17 is that it could be assumed that the horizontal flames had a virtual origin behind the rear of the corridor to allow for the vertical portion of the flames between the burner and the ceiling. The intensity of radiation at a given distance (relative to the flame length) along the flame was always the same and over most of the flame length the intensity fell off exponentially with increasing distance.

5.14. Flame lengths

It is shown in Appendix 3 that the flame length can be reasonably correlated as a function of a dimensionless group having the form of a Froude number

$$l/d = f\left(m'/\rho_o\, g^{\frac{1}{2}}\, d^{3/2}\right)$$

where l is the horizontal flame length measured from the virtual origin.

d is the depth of the layer of hot gases.

m' is the rate of flow of town gas per cm width.

and ρ_o is the density of the ambient air.

This is similar to the function given by Thomas for vertical flames[6] except that the relevant dimension is the depth of the layer of hot gases rather than the width of the fuel bed. For these corridors, the expression reduces to

$$l/d = f\left(V_f \rho_f/\rho_o\, g^{\frac{1}{2}}\, d^{3/2}\right)$$

where V_f was the volume rate of flow of town gas

and ρ_f was its density.

The correlation is shown in Fig. 18. The flame lengths measured in the preliminary experiments have also been included, it was assumed that in those experiments the virtual origin was at the same position as in later experiments, viz. $x_o = 100$ cm. Where the flames were longer than the corridor the value of l was not known but a minimum value of l/d was calculated assuming the flames were just reaching the end of the corridor. These points are indicated in Fig. 18 by upward pointing arrows.

When $(m'/\rho_o\, g^{\frac{1}{2}}\, d^{3/2}) < 0.024$ with either no front end screen or a 15 cm deep front end screen fitted to the corridor, and when $(m'/\rho_o\, g^{\frac{1}{2}}\, d^{3/2}) < 0.018$ with a 23 cm deep front end screen

$$l/d = 220\left(m'/\rho_o\, g^{\frac{1}{2}}\, d^{3/2}\right)^{\frac{2}{3}}$$

i.e. l is independent of d and proportional to $m'^{\frac{2}{3}}$.

Thus under these conditions it is immaterial what dimension d represents. Although the theoretical analysis suggests that it should in fact be the layer depth the assumptions made are so wide that the analysis can only be regarded as valid if the "critical" values of $m'/\rho_o \, g^{\frac{1}{2}} \, d^{3/2}$ (above which the $\frac{2}{3}$ power law no longer holds) are independent of scale for geometrically similar corridors. The experimental evidence shows that if d is taken to be the layer depth the critical value is apparently independent of scale for the one situation where the scale effect was examined i.e. when there was no screen at the front end of the corridor.

The critical value of $m'/\rho_o \, g^{\frac{1}{2}} \, d^{3/2}$ corresponded to the transition from the air-rich to the fuel-rich regime. In the fuel-rich regime the rate of burning is controlled by entrainment into the layer which is approximately constant with distance from the burner and hence the flame length should be proportional to the rate of flow of town gas. There are insufficient measurements to confirm this.

5.15. Comparison between horizontal and vertical flame lengths

An expression[9] for the heights of flames rising vertically from fuel beds of different shapes is

$$L/D \simeq 40 \, (m''/\rho_o \, (gD)^{\frac{1}{2}})^{\frac{2}{3}}$$

where L is the flame height

D is the shorter dimension of the fuel bed

and m" is the burning rate per unit base area of fuel bed

i.e. the lengths of horizontal flames (measured from their virtual origin) are about $5\frac{1}{2}$ times greater than the lengths of vertical flames from the same fuel bed.

The measurements were not strictly comparable as the horizontal flame lengths were measured to the tips of the flames whereas the mean lengths of the vertical flames were measured, but they do show the large increase in flame length due to deflection by the ceiling. The effect of the difference in the method of measurement has been studied for vertical flames.

Measurements of the lengths to the tips of vertical flames from burners 1.2 by 0.3 metres and 1.2 by 0.15 metres were therefore made using a "streak" camera. To a first approximation over the range of experimental results

$$L_t/D = 280 \, m''/\rho_o \, (gD)^{\frac{1}{2}}$$

where L_t was the flame height measured to its tip and the two expressions are shown in Fig. 19 together with the expression for air rich horizontal flames.

The distance of the virtual origin of the horizontal flames behind the rear of the corridor, x_o, is related to the vertical flame length.

The position of the virtual origin does not appear to depend on the town gas flow rate, so that if the latter is adjusted until the tips of the vertical flame are just entering the layer of hot gases (flame length = h-d, the distance of the bottom of the layer above the burner) the equivalent horizontal flames would have a length x_o, the distance of the virtual origin behind the rear of the corridor. The value of $(h-d)/D$ for these experiments lie below the range of vertical flame lengths investigated, and generally extrapolation is unjustified. However, with the burner 120 cm beneath the ceiling the distance between the burner and the bottom of the layer of hot gases was 65 cm; then $(h-d)/D = 1.3$ which is not far beyond the range investigated. x_o then has a value of 3.2 metres compared with the value of 2.4 metres found in the experiments.

5.16. Heat transfer to ceiling

The heat transfer to the ceiling should to a first approximation follow the same pattern as the radiation downwards. Generally the heat transfer varied roughly exponentially with distance along the corridor although (as with downward radiation) it did not do this at high rates of flow of town gas when the burner was 37 cm beneath the ceiling.

In Fig. 20 H/H_o is plotted against X/l

where H was the rate of heat transfer to the ceiling

and H_o was the rate of heat transfer to the ceiling at the virtual origin, found by extrapolation to have a value of about 70 W/cm^2.

The rate of heat transfer to the ceiling, varied with gas flow and with the distance of the burner beneath the ceiling in the same way as the downward intensity of radiation, and the two heat transfer rates were of the same order. The variation of the rate of heat transfer with distance from the virtual origin is given by

$$H/H_o = \exp(-k'X/l)$$

where $H_o = 70$ W/cm^2 and $k' = 4.6$ (which are slightly larger than the corresponding figures for downward radiation) over most of the flame lengths, although near the flame tip there is an appreciable deviation from the exponential. The small difference between heat transfer

to the ceiling and radiation downwards, is probably due to the additional heat transfer to the ceiling by convection and to the fact that there was a background of heat radiation downwards from the hot ceiling, but little heat was radiated upwards from the cold floor.

The heat transfer to the ceiling immediately over the burner, will determine whether a flammable ceiling lining is likely to ignite and the time taken to ignite it. The heat transfer to the ceiling is shown as a function of the town gas flow rate in Fig. 21, the solid lines represent the above equation, which at low rates of gas flow holds even immediately over the burner. However the maximum possible rate of heat transfer appeared to be about 17 W/cm^2 which occurred when $(m'/\rho_o\, g^{\frac{1}{2}}\, d^{3/2}) \simeq 0.02$. This appears to be the most sensitive criterion for the transition from an air-rich to a fuel-rich regime. Any increase in the gas flow rate above that necessary to give a heat transfer rate of 17 W/cm^2 resulted in a decrease in the heat transfer to the ceiling. A similar maximum rate of heat transfer to the ceiling was found in other experiments using wood fuel.

When the burner was 37 cm beneath the ceiling and the gas flow rate was 300 cm^3/s per centimetre width of burner, the maximum rate of heat transfer to the corridor ceiling occurred about 1 metre away from the burner and was only about $3\frac{1}{2}$ W/cm^2. This form of distribution of heat transfer was observed in the experiments[10] at the Danish National Testing Laboratory in Copenhagen in 1962-3.

In those experiments with wood fuel m' $\simeq$ 1.8 g/s per cm width of corridor, d $\simeq$ 1.0 metre and

$$m'/\rho_o\, g^{\frac{1}{2}}\, d^{3/2} \simeq 0.045$$

i.e. much larger than for the experiments described in this report.

5.17. Heat loss through ceiling

The calculation of the heat loss through the ceiling at equilibrium is discussed in Appendix 1. Based on these calculations the heat loss is given by

$$H_c = 5.7 \exp(-2.9\, X/l) \quad W/cm^2$$

Only about a quarter of the heat falling on the ceiling was lost through it at equilibrium.

5.18. Heat balance

The rate of flow of sensible heat in the layer of hot gases (Q_l) through any plane perpendicular to the flow was given by

$$Q_l = Q_f - Q_r - Q_u$$

where Q_f was the rate of heat gain (from combustion) between the burner and the plane.

Q_r was the rate of heat loss by radiation between the burner and the plane.

Q_u was the rate of heat loss through the ceiling and screens up to the plane.

Q_r and Q_u were derived from the experimental data as described in Appendix 4.

In a few experiments detailed velocity measurements enabled Q_l to be calculated from the experimental data (Table 4) and the heat balance for these experiments is given in Table 8.

The difference between the sum of the rates of heat loss and the heat output of the town gas never exceeded 10 per cent. Beyond the tips of the flames these two quantities should have been equal. The agreement in Table 8 is satisfactory.

Even when the flames extended 5.6 metres from the rear of the corridor (7.0 metres from the virtual source) and the measuring point was 2.0 metres from the rear of the corridor (3.4 metres from the virtual source) the heat loss was not significantly less than the calorific value; thus most of the combustion must occur within the first half of the effective flame length.

Generally, detailed velocity measurements were not available, but the heat content of the layer of hot gases at the flame tips in the air-rich regime was deduced from the calorific value of the town gas and the other heat losses.

i.e. $$Q_l = Q_f - Q_r - Q_u$$

There were large variations in the relative importance of the various methods of heat dissipation both with the rate of flow of town gas and the distance of the burner beneath the ceiling. However for geometrically similar flames it would be expected that the percentage of the heat input dissipated by each method should be independent of scale. A shape factor may be defined as (horizontal flame length)/(total flame length) i.e. $(1 - x_o)/1$ and the heat losses have been plotted as a function of this

Table 8

Heat balance from heat transfer measurements

Burner 66 cm beneath ceiling

(All heat flow rates refer to a 1 cm width of corridor)

Gas flow per cm width cm^3/s	Horizontal flame length m	Distance of measuring point from rear of corridor m	Heat loss				
			Radiation Q_r kW	Through ceiling and walls Q_u kW	In stream of hot gases Q_l kW	Total Q_f kW	Heat output from town gas kW
300	5.6	2.0	1.8	0.8	2.0	4.6	5.0
		5.2	2.7	1.2	1.5	5.4	
183	3.6	2.0	1.1	0.6	1.6	3.3	3.0
		5.2	1.4	0.8	1.0	3.2	
83	1.3	2.0	0.22	0.21	0.84	1.3	1.4
		5.2	0.24	0.23	0.80	1.3	

in Figs. 22 and 23. Except where the burner was 37 cm below the ceiling with a gas flow rate of 83 cm^3/s per cm width, the percentage heat losses do appear to be independent of scale. The reason for the anomalous behaviour in the one particular experiment is not clear since there is no doubt that the layer was air-rich in that instance, and the behaviour at a higher town gas flow was not anomalous.

As the length of the horizontal portion of the flames increased the proportion of the heat input which was radiated into the corridor also increased, from about 15 to 55 per cent in these experiments. At the same time the loss through the ceiling and walls increased from 10 to 25 per cent while the heat content of the hot gas layer decreased from 75 to 20 per cent.

Although further radiation will occur beyond the flame tips the fraction which occurs up to the flame tips is a measure of the fraction which is at a sufficiently high intensity to cause spread of flame over surfaces. Thus, as a fire grows in size so that the horizontal flames become larger, not only is more heat produced but a greater part of that heat is radiated at an intensity sufficient to cause flame spread.

5.19. Effect of emissivity on heat balance

The effect of the emissivity of the layer of hot gases on the heat balance can only easily be considered very approximately.

It is assumed that the layer of hot gases and flames was radiating as a uniform grey body of emissivity ε and that heat transfer to the ceiling by convection could be ignored in comparison with radiative transfer. Two limiting types of ceilings are considered, firstly a perfectly insulating ceiling, in which all the heat absorbed by the ceiling is re-radiated.

Then $\varepsilon \sigma T^4 = \sigma T_c^4$

where T was the absolute hot gas temperature

and T_c was the absolute ceiling temperature

For the heat balance of the layer at equilibrium

$$\varepsilon \sigma T^4 + (1 - \varepsilon) \sigma T_c^4 + B\dot{Q} + \dot{L} = Q$$

where $B\dot{Q}$ was the increase in the sensible heat

$\dot{L}$ was the increase in the heat carried as latent heat in the water vapour (due to the increase in the mass of water vapour resulting from combustion) per unit area of ceiling

and Q was the heat output of the burning fuel per unit area of ceiling.

Combining the above two equations gives:-

$$(2\varepsilon - \varepsilon^2)\sigma T^4 + B\Theta = Q - A$$

Assuming $Q = 7.5$ W/cm^2, $A = 1.0$ W/cm^2 and $B = 3.3 \times 10^{-2}$ W cm^{-2}deg C^{-1} the effect of ε on the downward radiation has been plotted in Fig. 24.

The second case is that of a cold ceiling assuming all heat falling on it is absorbed.

Then, for the heat balance of the layer,

$$2\varepsilon\sigma T^4 + K\Theta = Q - A$$

For the same heat output as before the effect of ε on the downward radiation has also been plotted in Fig. 24. A reduction in emissivity from unity to 0.5 with a cold ceiling or 0.3 with a perfectly insulating ceiling results in a reduction in downward radiation of only 10 per cent.

6. CONCLUSIONS

(1) Two regimes of burning could be distinguished, one in which the layer of hot gases beneath the ceiling was air-rich and one in which it was fuel-rich. In the air-rich regime the layer contained more than sufficient air (mainly derived from entrainment by the vertical portion of the flames) for complete combustion of the town gas; the rate of combustion was then presumably controlled by mixing within the layer and flames were generally close to the ceiling.

In the fuel-rich regime the rate of combustion was controlled by the limited entrainment into the base of the layer and flames were confined to the lower part of the layer.

Because entrainment both into the vertical flames and into the base of the layer occurred simultaneously the transition from one regime to the other was not well defined.

It is likely that with an actual fire in a compartment the air-rich regime would be important during the critical stages in its growth.

(2) The horizontal flames behaved as though they originated from a virtual source at a distance x_o behind the rear screen; x_o depended on the distance of the burner beneath the ceiling but did not depend on the rate of flow of town gas.

(3) The horizontal flame lengths measured from the virtual source could be correlated by the relationship $l/d = f\,(m'/\rho_o\, g^{\frac{1}{2}}\, d^{3/2})$. The transition from the air-rich to the fuel-rich regime occurred at a critical value of $(m'/\rho_o\, g^{\frac{1}{2}}\, d^{3/2})$ of about 0.025 if the front end was open but rather less if it was partly closed by a screen.

In the air-rich regime

$$l/d = 220\ (m'/\rho_o\ g^{\frac{1}{2}}\ d^{3/2})^{\frac{2}{3}}$$

$$\therefore \quad l = 220\ (m'/\rho_o)^{\frac{2}{3}}/g^{\frac{1}{3}}$$

Above the critical value the flames became further elongated.

(4) If distances along an air-rich flame measured from the virtual origin were scaled according to the flame lengths, then the intensity of radiation downwards at a given distance from the virtual origin was always the same whatever the town gas flow or the distance of the burner beneath the ceiling. Over most of the flame length

$$I = 50 \exp(-4.05\ X/l)\ W/cm^2$$

When the layer was fuel-rich the intensity near the rear of the corridor was less while that near the front end was greater than would be calculated from the above formula.

(5) The heat transfer to the ceiling obeyed similar laws to the downward radiation and in the air-rich regime over most of the flame length

$$H = 70 \exp(-4.6\ X/l)\ W/cm^2$$

The heat transfer to the ceiling immediately over the burner had a peak value of 17 W/cm^2 which occurred slightly before the other signs of the transition from an air-rich to a fuel-rich layer (i.e. when $m'/\rho_o\ g^{\frac{1}{2}}\ d^{3/2}$ was slightly less than the critical value given in (3) above). In the fuel-rich regime the heat transfer to the ceiling immediately over the burner decreased with increasing town gas flow.

(6) The heat loss by radiation into the corridor up to the flame tips is a measure of the proportion of the heat of combustion which is radiated at an intensity sufficient to cause flame spread over materials. In the air-rich regime this depended on a shape factor defined as $(l - x_o)/l$ and increased from about 15 per cent when this was 0.5 to 55 per cent when it was about 0.8.

(7) The above relationships have been established for the experimental corridor (which was effectively without a floor). Differences in the emissivity of the flames should not be of great importance and there was no evidence of a scale factor, so that it should be possible to use the relationships for larger scales although larger scale experiments are obviously desirable. Although experiments were carried out with one burner width only,

the form of the correlation for flame length suggests that the results should apply to other burner widths or to fires of the same order of size. Changing the insulation of the corridor would not be expected to change the form of the above relationships although the values of heat transfer rates would be altered. The effect of a floor to the corridor will be discussed in a further report.

7. ACKNOWLEDGEMENT

The authors wish to thank Miss A. Wadley for her able assistance with the experimental work.

8. REFERENCES

(1) HIRD, D. and FISCHL, C. F. Fire hazard of internal linings. Department of Scientific and Industrial Research and Fire Offices' Committee National Building Studies Special Report No. 22, London, 1954, H.M.S.O.

(2) HESELDEN, A. J. M. Fully developed fires in a single compartment, Part 1 Apparatus and measurement methods for experiments with town gas fuel. Joint Fire Research Organization F.R. Note No. 555, 1964.

(3) McGUIRE, J. H. and WRAIGHT, H. Radiometer for field use. J. Sci. Instrum 1960, 37, 128-30.

(4) HINKLEY, P. L. and HESELDEN, A. J. M. An improvement to a radiometer for field use. J. Sci. Instrum. 1963, 40, 379.

(5) HESELDEN, A. J. M. An instrument for measuring total heat fluxes within flames. Joint Fire Research Organization F.R. Note No. 531, 1963.

(6) THOMAS, P. H. The size of flames from natural fires. Ninth International Symposium on Combustion. New York, 1963, Academic Press Inc.

(7) ROGERS, E. W. E. Encyclopaedic Dictionary of Physics, Oxford 1962, 5 515 Pergamon Press.

(8) THOMAS, P. H. and HINKLEY, P. L. et al. Investigations of the flow of hot gases in roof venting. Department of Scientific and Industrial Research and Fire Offices' Committee Joint Fire Research Organization Fire Research Technical Paper No. 7, London, 1963, H.M. Stationery Office.

(9) THOMAS, P. H., SIMMS, D. L. and WRAIGHT, H. G. H. Flames from fire fronts of different shapes. Joint Fire Research Organization F.R. Note No. 579, 1964.

(10) CHRISTENSEN, G. LOHSE, U. and MALMSTEDT, K. Full scale fire tests. Danish National Institute of Building Research S.B.I. Report No. 59, 1967.

(11) BURKE, S. P. and SCHUMANN, T. E. W. Diffusion flames Industrial and Engineering Chemistry 1928, 20 (10), 998-1004.

APPENDIX 2

Radiation intensity at base of hot gas layer and radiometer readings

The intensity of radiation at the base of the layer of hot gases varied with distance from the burner but at any given distance it was approximately constant across the width of the corridor.

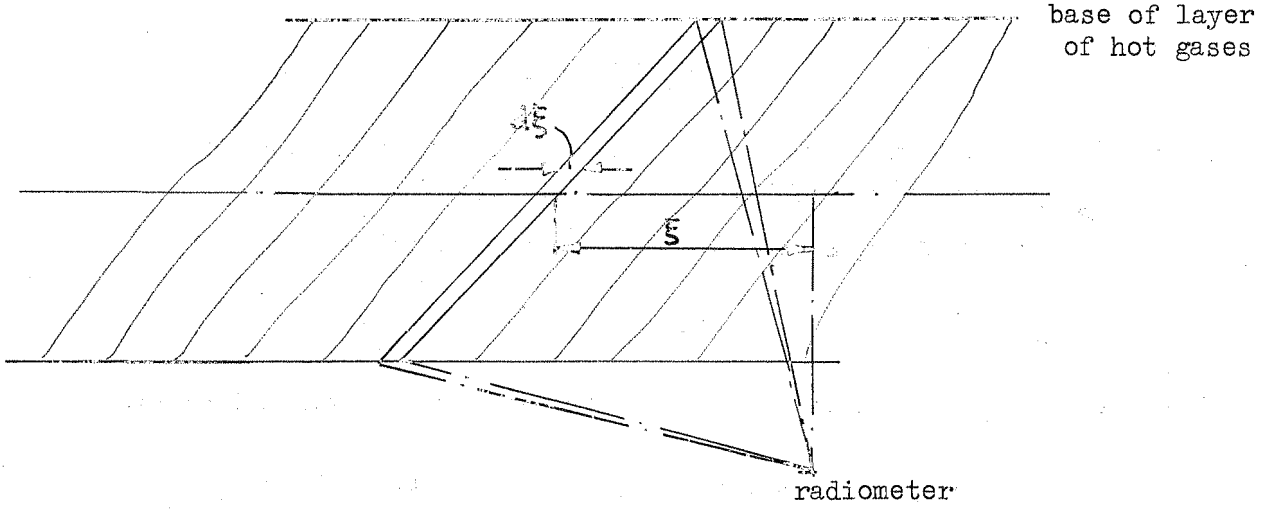

Consider a narrow strip of the base of the layer of hot gases normal to the axis of the corridor and a distance ξ from the point immediately above the radiometer. If $\phi(\xi)$ was the configuration factor of this strip at the radiometer, the total intensity of radiation at the radiometer (I_r) was given by

$$I_r = \int_{\xi = -a}^{\xi = a} I(\xi)\,\phi(\xi)$$

where $I(\xi)$ was the intensity of radiation from the strip. This expression may be easily evaluated for two cases.

Case 1

If the radiation varied linearly along the corridor the radiation received by the radiometer was the same as it would have been if the bottom of the layer of hot gases was radiating uniformly at the intensity immediately above the radiometer (I_c) because the radiation received varies linearly with that

emitted, i.e.

$$I_r = I_c \, \phi_a$$

where ϕ_a was the configuration factor at the radiometer of the position of the bottom of the layer of hot gases within the limits of "cut-off" of the radiometer.

Case 2

If

$$I = I_o \exp(-kX)$$

where I was the intensity at any point along the corridor
I_o was the intensity at the virtual origin
X was distance measured from the virtual origin

$$I_c = I_o \exp(-kx_r)$$

where x_r was the distance of the radiometer from the virtual origin

$$I(\xi) = I_o \exp -k(x_r + \xi) = I_c \exp(-k\xi)$$

$$I_r = I_c \sum_{\xi=-a}^{\xi=a} \exp(-k\xi)\, \phi(\xi) \qquad \ldots.(2.1)$$

The summation term is independent of x_r and thus, if the radiation distribution at the radiometer was exponential, the radiation distribution at the bottom of the layer of hot gases must also have been exponential.

Equation (2.1) may be written

$$I_r = I_c \, \phi_a \, /K$$

where K is a function of k.

Approximate values of K were evaluated (Table 9) for the values of k obtained in the experiments.

Table 9

Correction factors for radiation

Gas flow cm^3/s per cm width	K
300	0.99
125	0.95
83	0.90

Thus at high gas flows

$$I_r = I_c \phi_a$$

with an error which was negligible compared with uncertainties in measurement. The maximum error was 10 per cent at the lowest gas flow.

APPENDIX 3

Horizontal flame lengths

Thomas[6] has shown that data on flames rising vertically from a fire can be related approximately to data obtained from studies of non-reacting hot gases.

He has shown that for any fuel the height of a turbulent diffusion flame L is related to the volumetric flow of fuel per unit area of burner V_f'' and the burner dimension D

$$L/D = f\left(V_f''/(gD)^{\frac{1}{2}}\right)$$

or

$$L/D = f\left(m''/\rho_\infty (gD)^{\frac{1}{2}}\right)$$

where m'' is mass rate of flow of fuel per unit area of burner

or for a line source

$$L/D = f\left(V_f^2/gD^3\right)$$

Thomas's analysis can be adapted for horizontal flames and since the main basic assumptions are the same for both vertical and horizontal flames the resulting correlations should be equally valid.

It is assumed that the layer of hot gases beneath the ceiling contains air which has been entrained by the vertical portion of the flames from the burner but that no further entrainment takes place between the layer and the cool air beneath.

By analogy with fluid flow in channels the flame length was assumed to be controlled by turbulent mixing within the layer itself. The Reynolds number in the experiment (taking the characteristic dimension as the depth of the layer of hot gases) was of the order of 10,000.

The fuel gas and air were already partly mixed when they reached the ceiling and it is assumed that this mixing is equivalent to that which would have taken place had the layer originated from streams of unmixed gas and air at a distance x_o behind the rear of the model (Fig 26) i.e. the upper part of the stream at the virtual origin was a layer of fuel gas of depth d_f.

This problem has been solved for the laminar condition by Burke and Schumann[11] whose results lead to an equation for the flame length for a given fuel of the form

$$cl/\rho_\infty d^2 = f_1\ (d_f/d) = f_1\ (V_f/V)$$

where

c	is the molecular diffusion coefficient
u_1	is velocity of the flames
l	is the flame length
V_f	is the volume rate of flow of fuel gas
V	is the volume rate of flow of air and fuel gas

For the turbulent condition c would be replaced by the eddy diffusivity which in this situation may be regarded as proportional to vd

and $$l/d \propto f_1 \ (V_f/V) \qquad \ldots\ldots (3.1)$$

However, V and d are generally not independent; if the depth of the layer of hot gases is governed by the flow over the end of the model

$$V^2 \propto gd^3 \qquad \ldots\ldots (3.2)$$

and equation (3.1) becomes

$$l/d = f_2(V_f^2/gd^3) \qquad \ldots\ldots (3.3)$$

Alternatively, if the depth of the layer is partly controlled by the upward momentum of the hot gases rising from the fire, it follows that, since the gases in the layer consist mainly of air entrained in the vertical portion of the flames,

$$V \propto (h - d)^{3/2} \ g^{\frac{1}{2}}$$

but from Fig 12

$$d \propto h$$

i.e. $$V^2 \propto gd^3 \text{ as in equation (3.2)}$$

which again leads to equation (3.3).

If the front end of the model is partly obstructed by a screen, d in equation (3.2) is the depth measured from the bottom edge of the screen and hence the form of the functional relationships (f_2) will depend on screen depth (d_s)

i.e. $$l/d = f_4 \ (V_f^2/gd^3 \ , \ d/d_s)$$

When V_f/V is greater than the stoichiometric ratio, i.e. $V_f/(gd^3)^{\frac{1}{2}}$ is greater than a critical value, the flames will pass from the air-rich to the fuel-rich regime.

APPENDIX 4

Heat balance calculation for hot gas layer from experimental results

The heat balance of the layer of hot gases up to any plane perpendicular to the flow is given by

$$Q_f = Q_r + Q_l + Q_u$$

where Q_f is the rate of heat output due to combustion up to that point

Q_r is the rate of heat loss by radiation up to the same point

Q_u is the rate of heat loss through the ceiling and screens

and Q_l is the rate of flow of heat contained in the hot gases passing through the plane

Q always refers to a unit (1 cm) width of corridor.

Radiation loss

$$Q_r = Q_{r1} + Q_{r2} - Q_{r3} - Q_{r4}$$

where Q_{r1} is the radiation from the horizontal flames

Q_{r2} is the radiation from the vertical flames

Q_{r3} is the radiation from the horizontal flames intercepted by the vertical flames

and Q_{r4} is the radiation from the vertical flames intercepted by the horizontal flames

Since $I = 50 \exp(-4.05\, X/l)$ W/cm^2

$$Q_{r1} = 12.3\, l \left[\left(\exp(-4.05\, X/l\right) - \exp\left(-4.05\, (x_o + 50)/l\right) \right]$$

where $x_o + 50$ was the distance of the front of the burner from the virtual origin

$$Q_{r2} = I_v h$$

where I_v was the radiation intensity from the vertical flames measured by the pyrometer, Fig 8.

$$Q_{r3} = \int_{x_o+50}^{X} I\, \phi(x)\, dx$$

where $\phi(x)$ was the configuration factor of a strip dx of the horizontal flames relative to the vertical flames, this was evaluated graphically in a few instances.

$$Q_{r4} = \phi_v \, I_v \, h$$

where ϕ_v was the configuration factor of the vertical flames relative to the horizontal. It was found that $Q_{r4} \simeq Q_{r3}$.

Loss through ceiling and screens

$$Q_u = Q_{u1} + Q_{u2} + Q_{u3}$$

where Q_{u1} was the heat loss through the ceiling

Q_{u2} was the heat loss through the side screens

and Q_{u3} was the heat loss through the rear screen

Since $H_c = 5.7 \exp(-2.9 X/l)$ W/cm^2

$$Q_{u1} = 20.1 \left(\exp(-2.9 X/l) - \exp(-2.9 x_o/l)\right)$$

It was assumed that heat was lost through the side screens at the same rate as through the ceiling, i.e. $Q_{u2} = Q_{u1} (2d/\omega)$.

The heat lost through the rear screen was regarded as similar to the heat lost through the ceiling

i.e. $$Q_{u3} = 0.4 \, h \, I_v^{0.63}$$

Heat content of the layer

Q_I was derived as described previously by graphical integration of the velocity profiles in Fig 14.

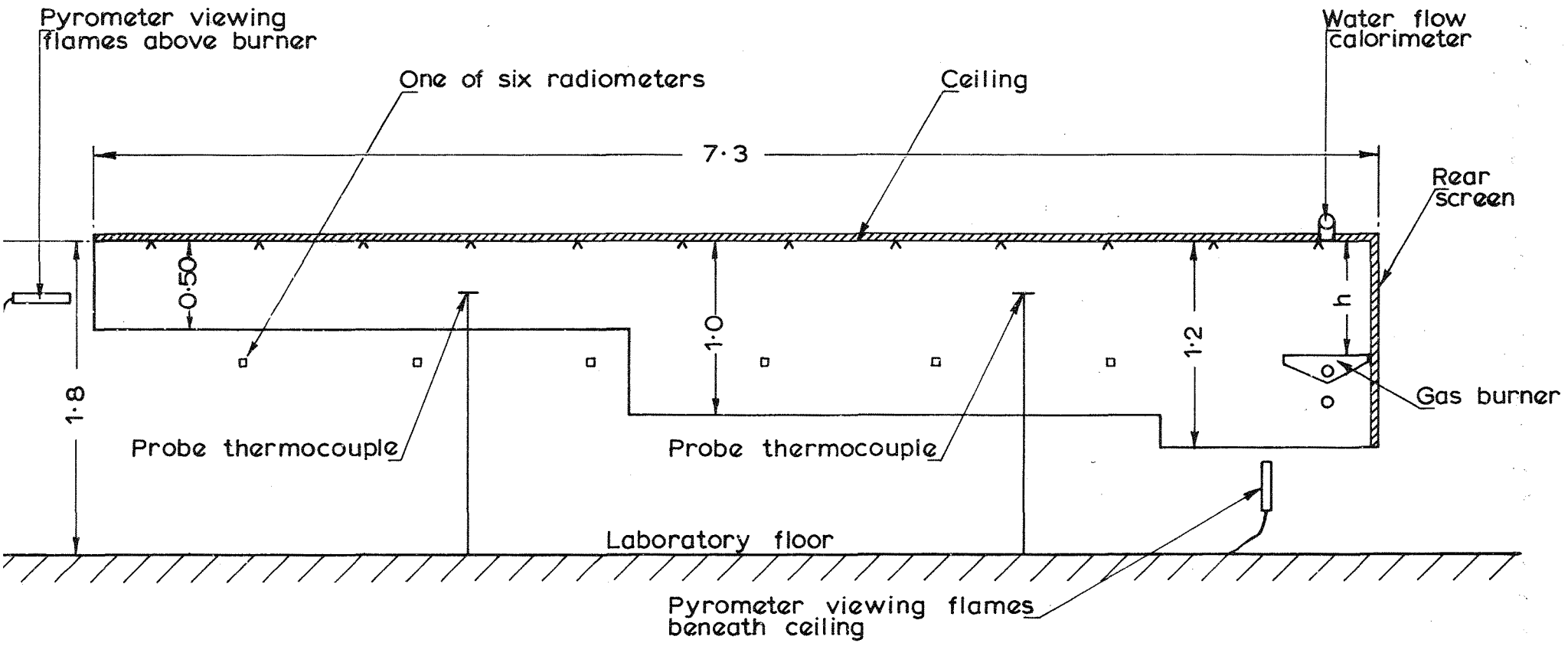

All dimensions in metres
12 ceiling thermocouples shown thus

FIG. 1. DIAGRAM OF MODEL CORRIDOR

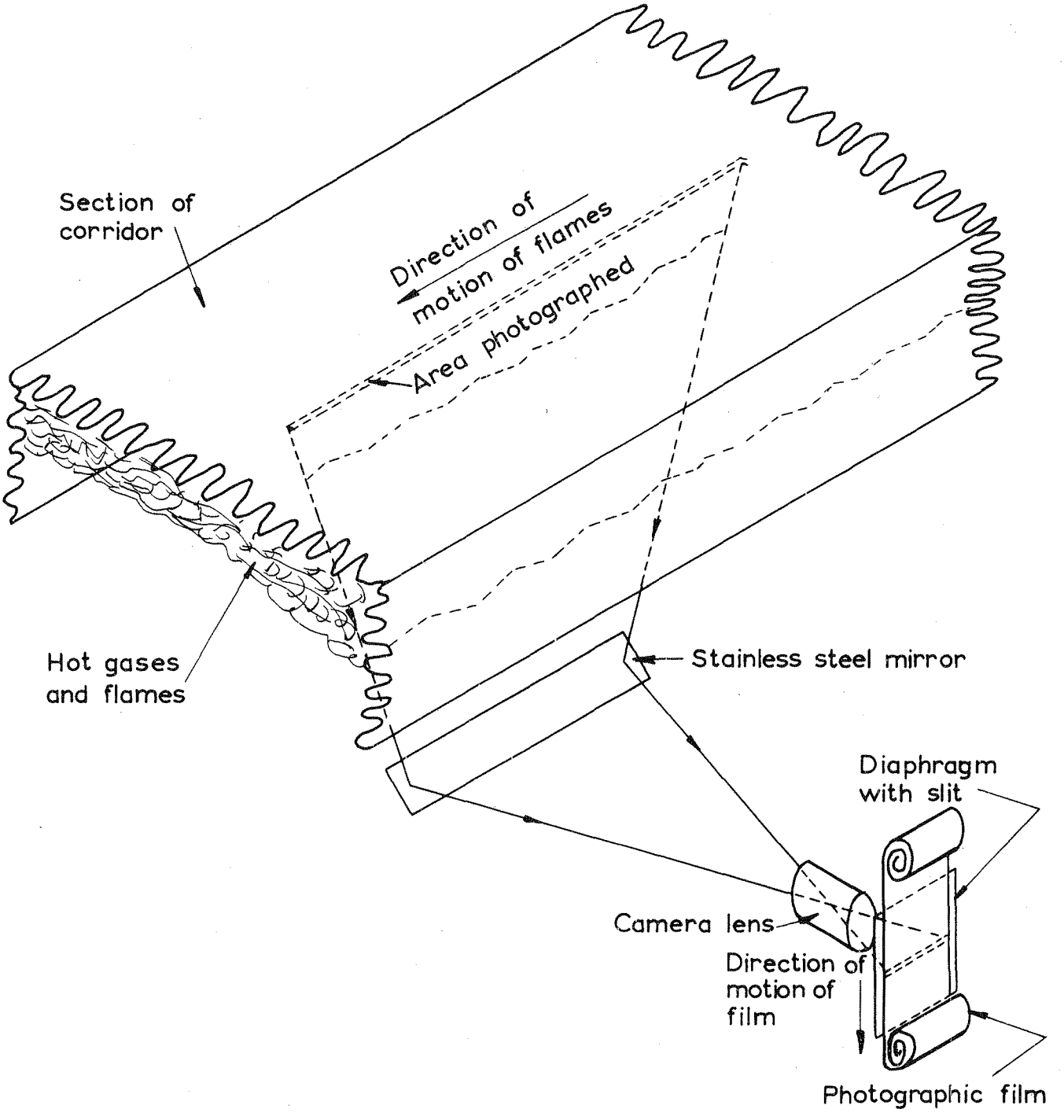

FIG. 2. ISOMETRIC DIAGRAM OF APPARATUS FOR MEASURING VELOCITY OF LUMINOUS FLAMES

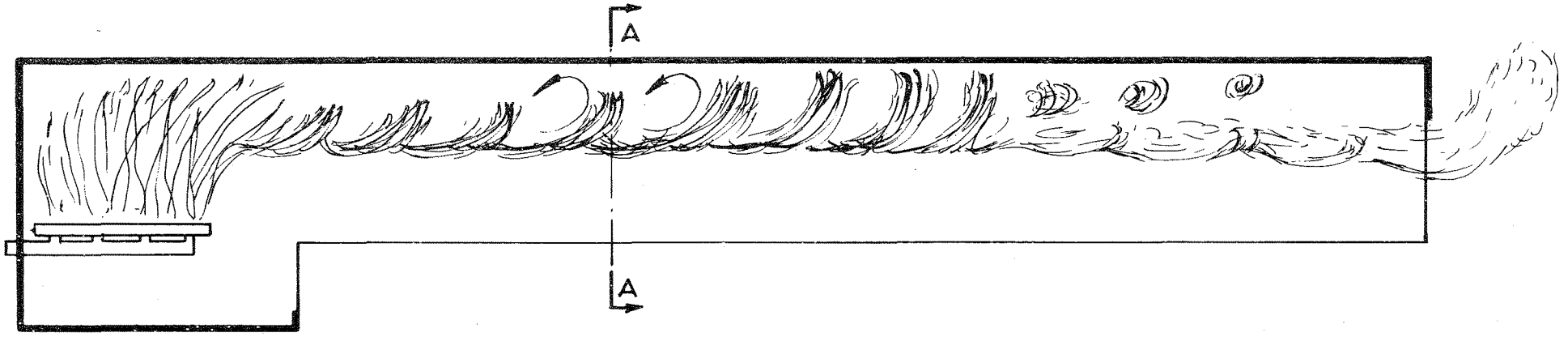

(a) LONGITUDINAL SECTION

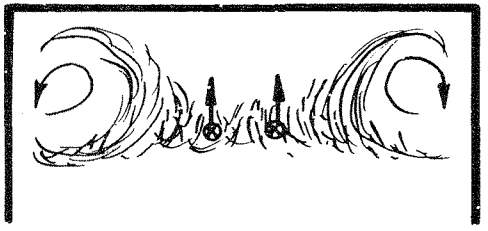

(b) TRANSVERSE SECTION A-A

Not to scale

Rate of flow of fuel gas – c200 cm ^{3}/s per cm width of corridor

FIG. 3. DIAGRAM SHOWING GENERAL APPEARANCE OF FLAMES EARLY MODEL 5·8m LONG

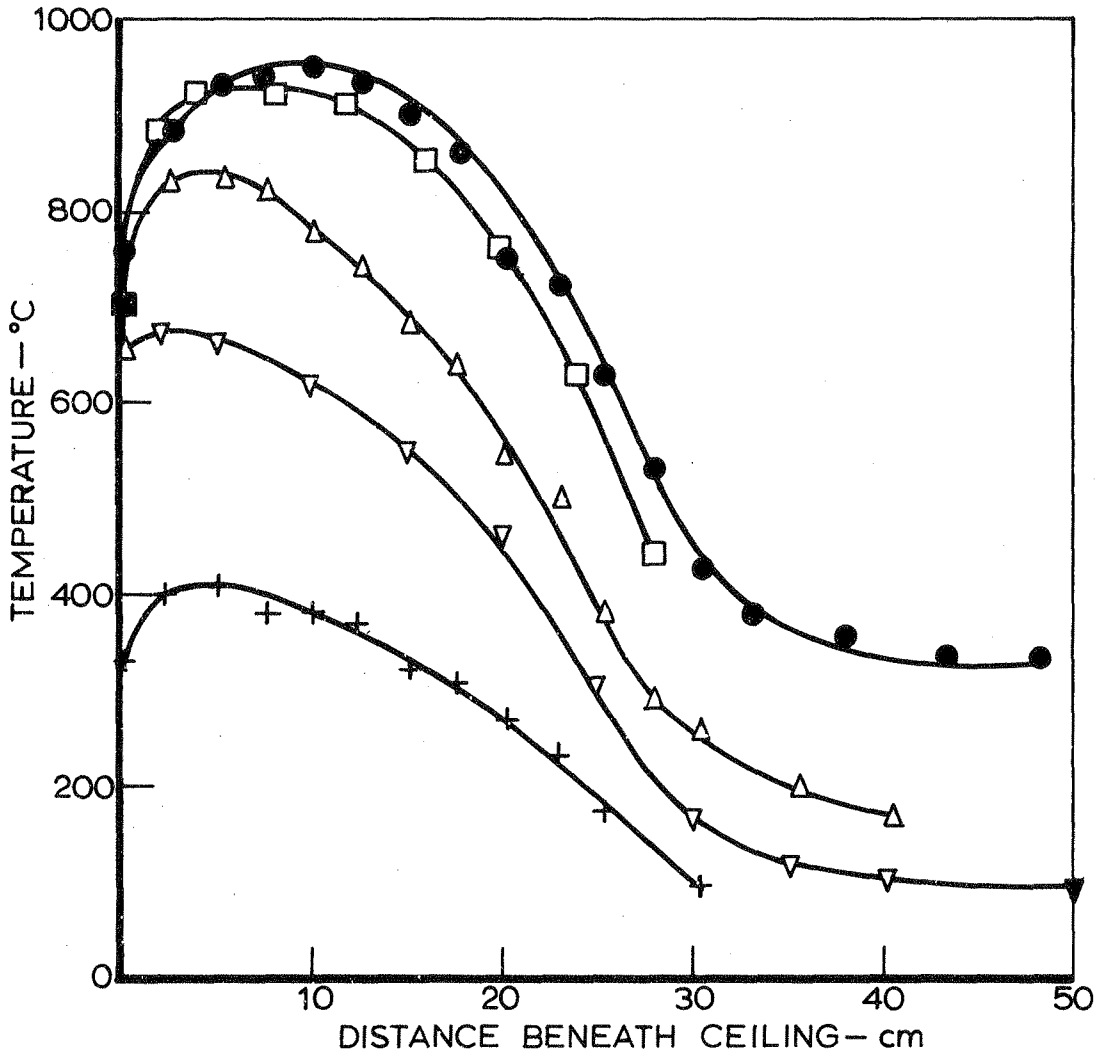

Symbol	Gas flow per cm width cm^3/s
●	300
□	250
Δ	183
▽	125
+	83

Burner 66 cm beneath ceiling

FIG. 4. TYPICAL VERTICAL TEMPERATURE DISTRIBUTION— EFFECT OF GAS FLOW 2m FROM REAR OF CORRIDOR

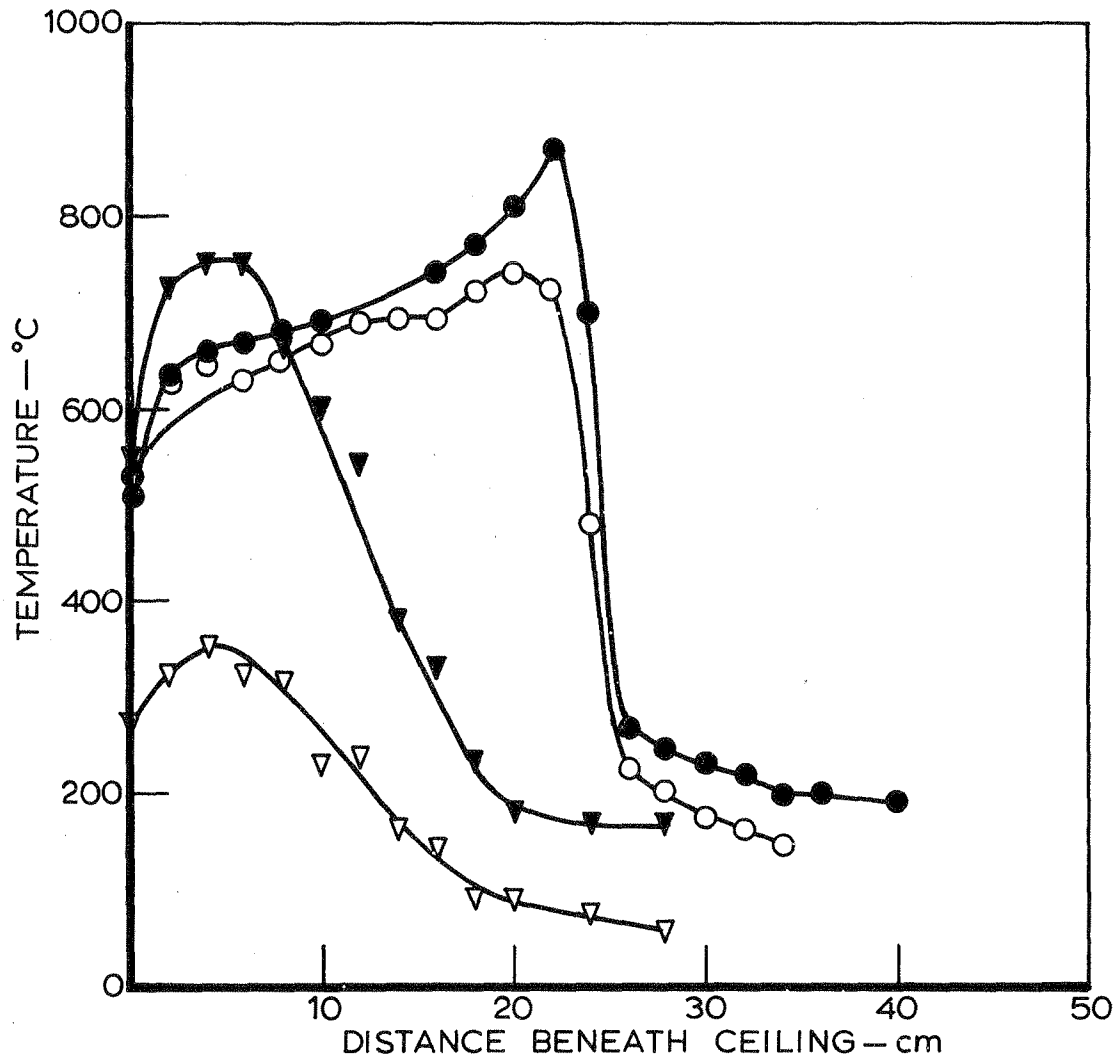

Symbol	Gas flow cm^3/s per cm width	Distance from rear of corridor m
Fuel-rich ● flames ○	300	2·0 5·2
Air-rich ▼ flames ▽	125	2·0 5·2

Burner 37 cm beneath ceiling

FIG. 6. TYPICAL VERTICAL TEMPERATURE DISTRIBUTION — EFFECT OF DISTANCE FROM REAR OF CORRIDOR

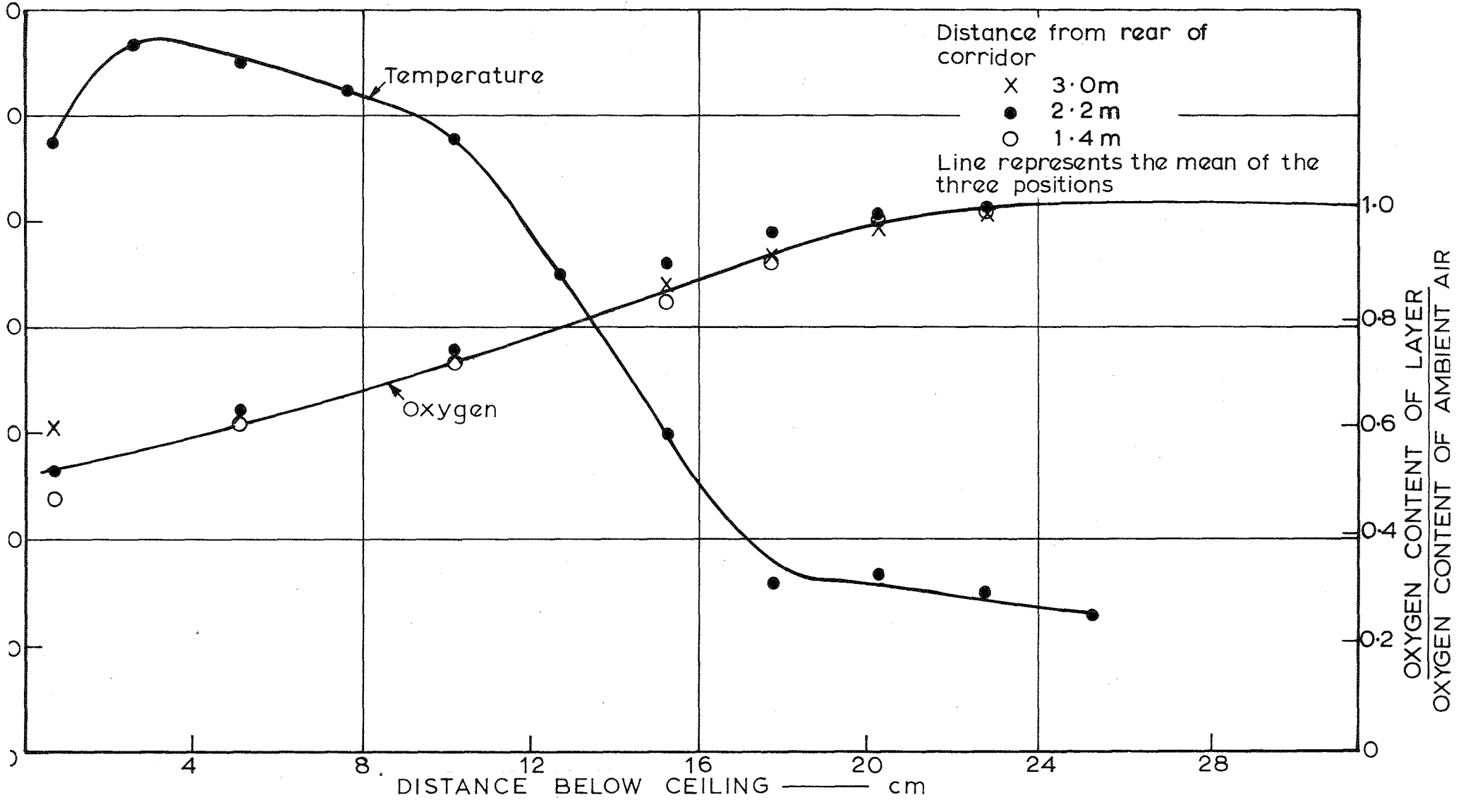

TEMPERATURE AND OXYGEN CONCENTRATIONS IN LAYER — LOW RATES OF FLOW OF TOWN GAS — 50 cm^3/s PER cm WIDTH OF CORRIDOR

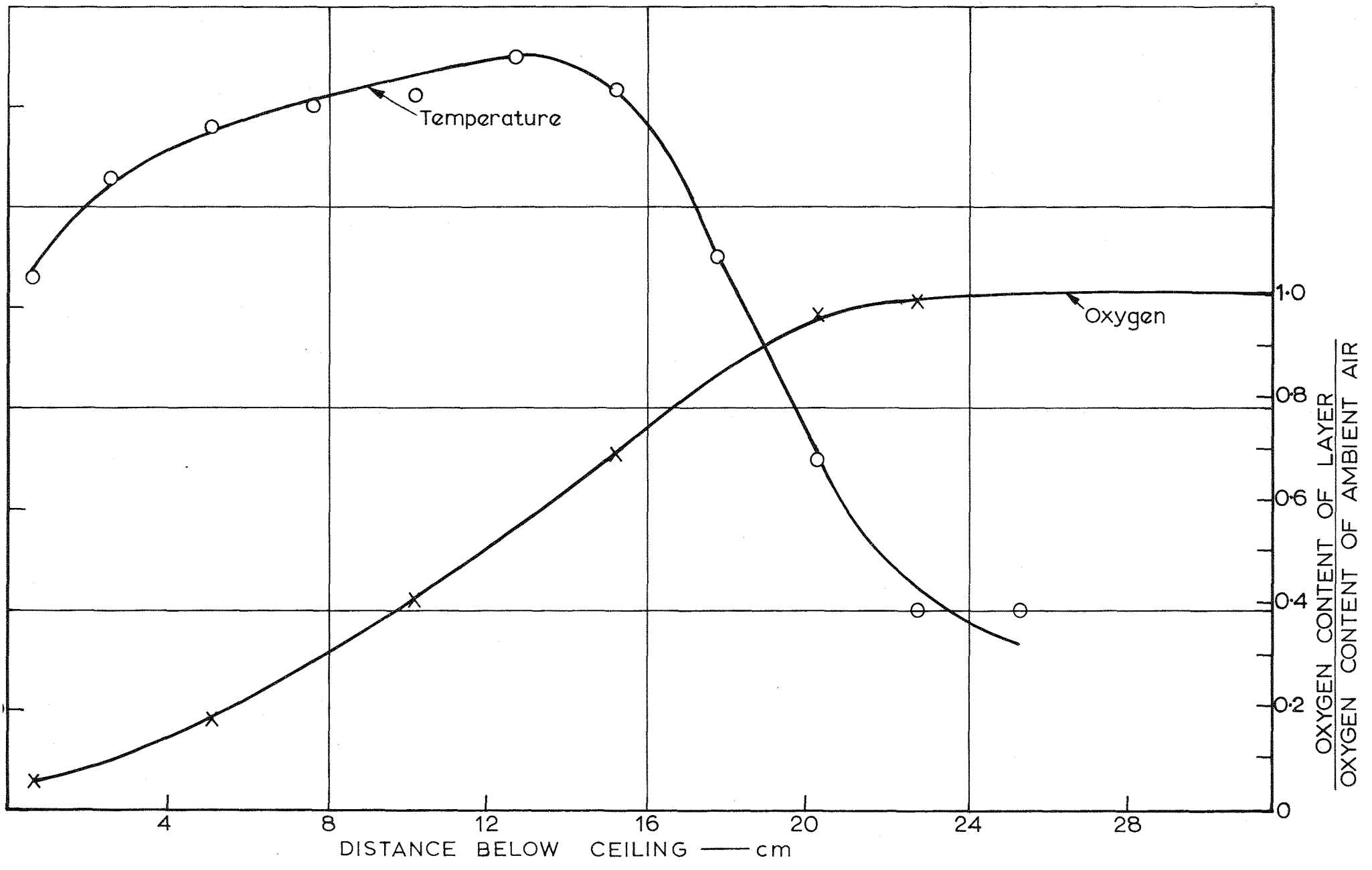

EMPERATURE AND OXYGEN CONCENTRATIONS IN LAYER — INTERMEDIATE RATES OF _OW OF TOWN GAS - 135 cm^3/s PER cm WIDTH OF CORRIDOR

381 FR72

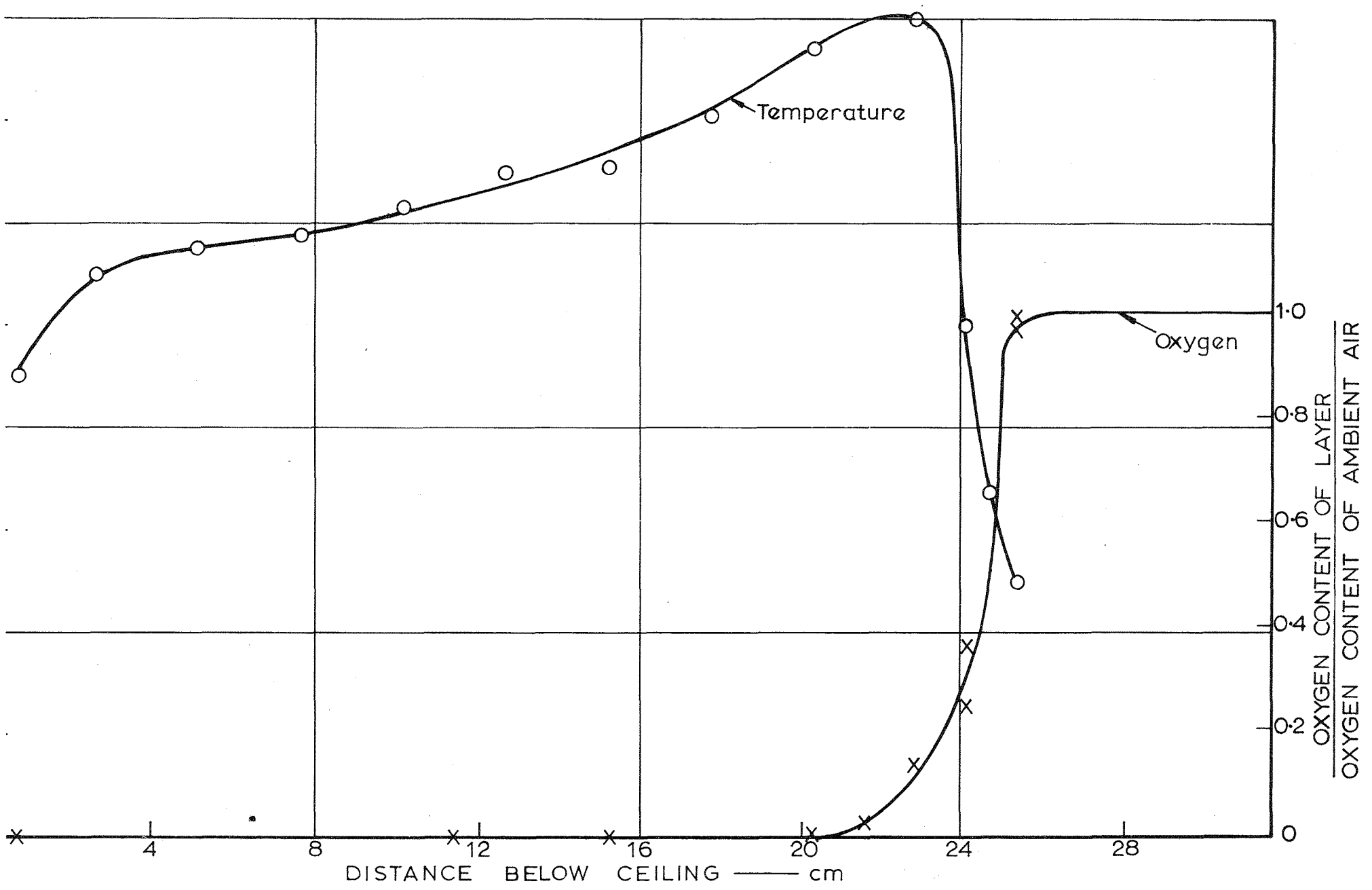

EMPERATURE AND OXYGEN CONCENTRATIONS IN LAYER — HIGH RATES OF FLOW
)F TOWN GAS — 340cm^3/s PER cm WIDTH OF CORRIDOR

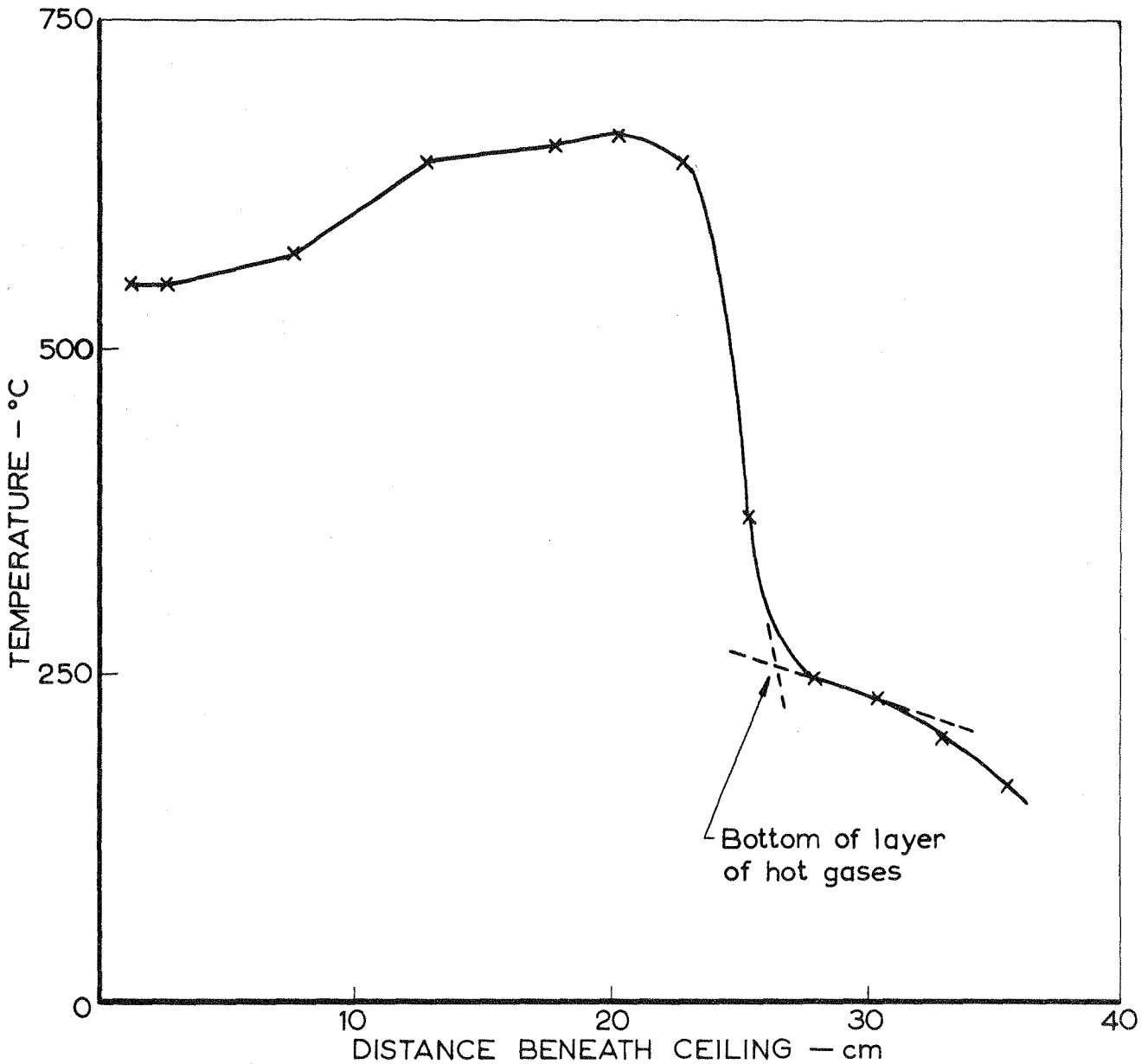

FIG. 10. DEFINITION OF BOTTOM OF LAYER OF HOT GASES

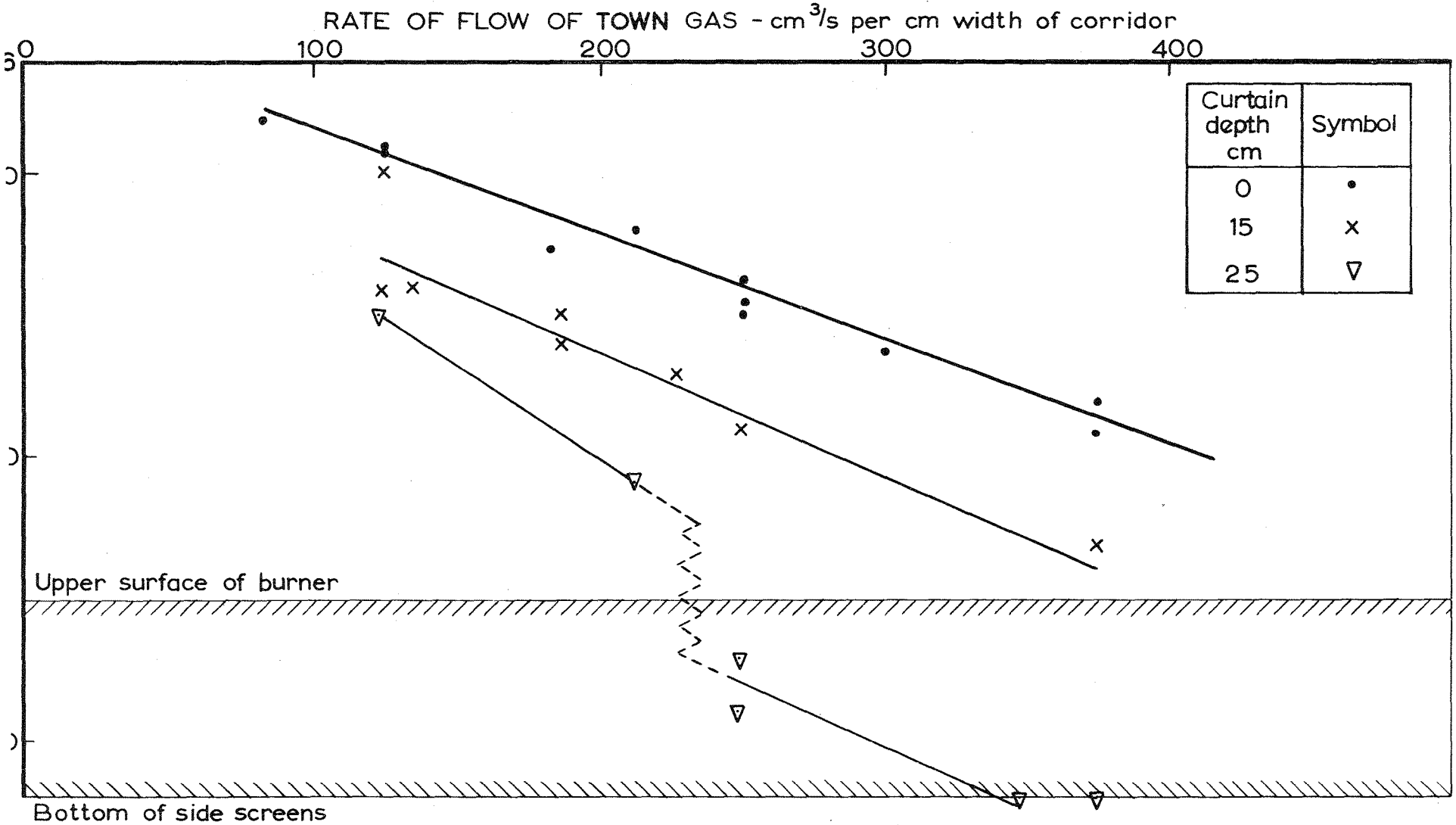

FIG. 11. DEPTH OF LAYER OF HOT GASES

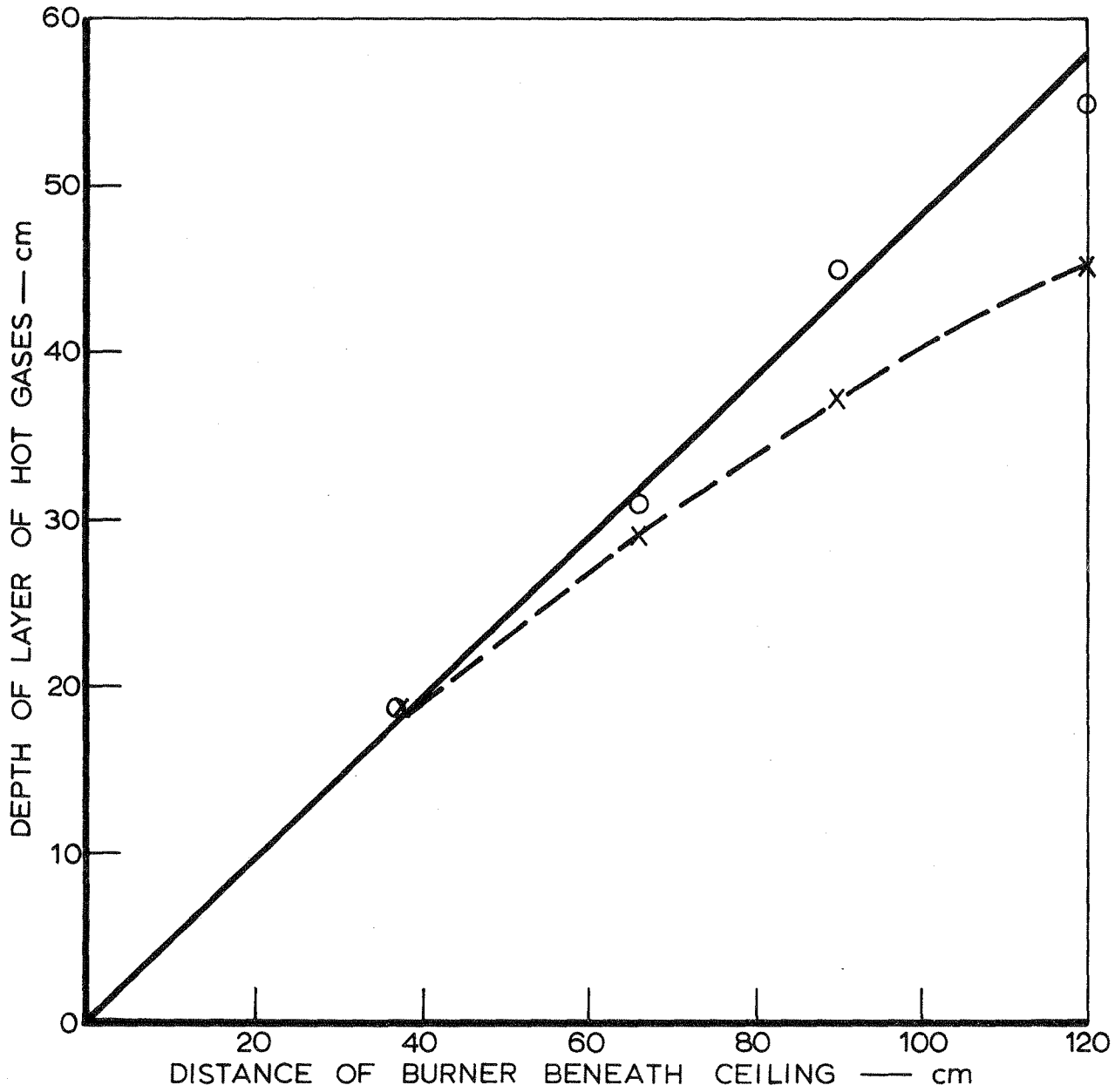

Symbol	Depth measured from rear m
—— O	2·0
— — X	5·2

FIG. 12. LAYER DEPTH AS A FUNCTION OF DISTANCE OF BURNER BENEATH CEILING (NO SCREEN AT

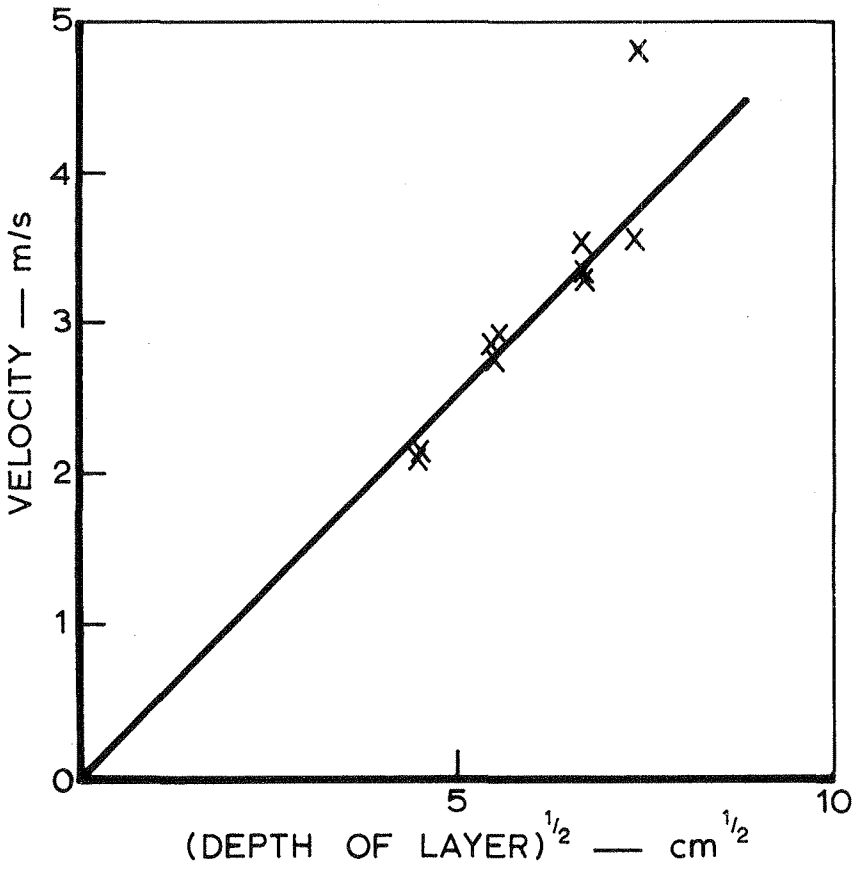

FIG. 13. VELOCITY OF LUMINOUS FLAMES (2·0m FROM REAR, AIR-RICH REGIME) AS A FUNCTION OF DEPTH OF LAYER OF HOT GASES

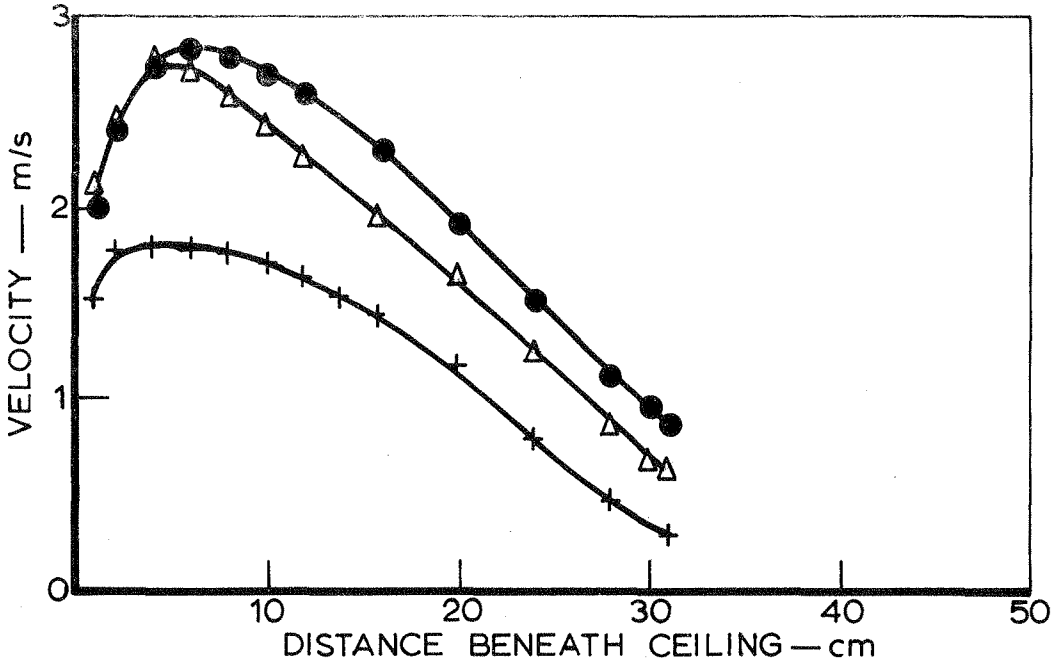

(a) 2·0m from rear of corridor

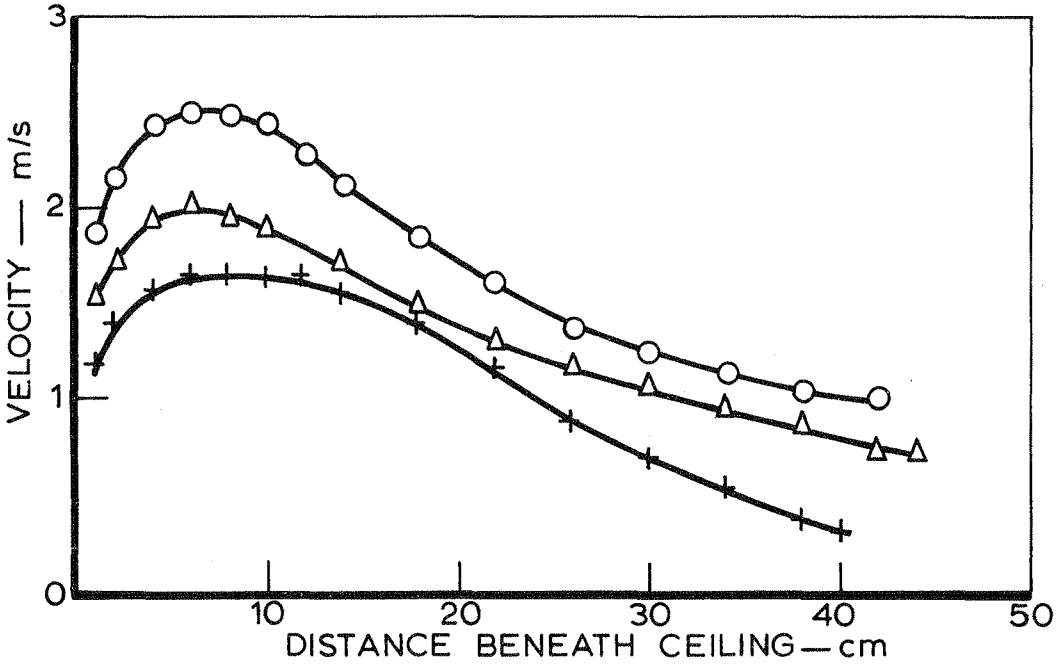

(b) 5·2m from rear of corridor

Symbol	Gas flow per cm width cm^3/s
● O	300
Δ	183
+	83

Burner 66 cm beneath ceiling

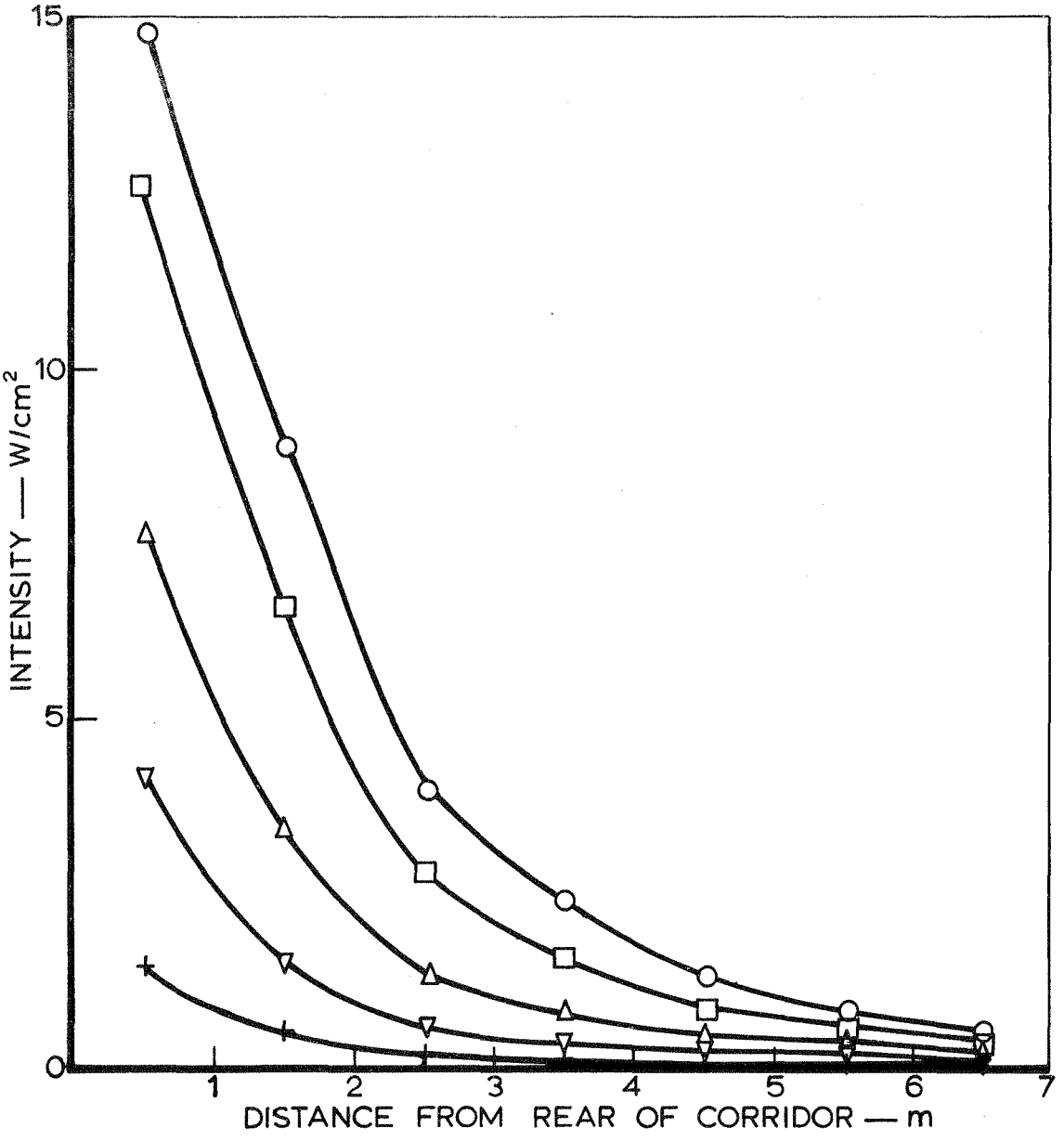

(a) Burner 90 cm beneath ceiling

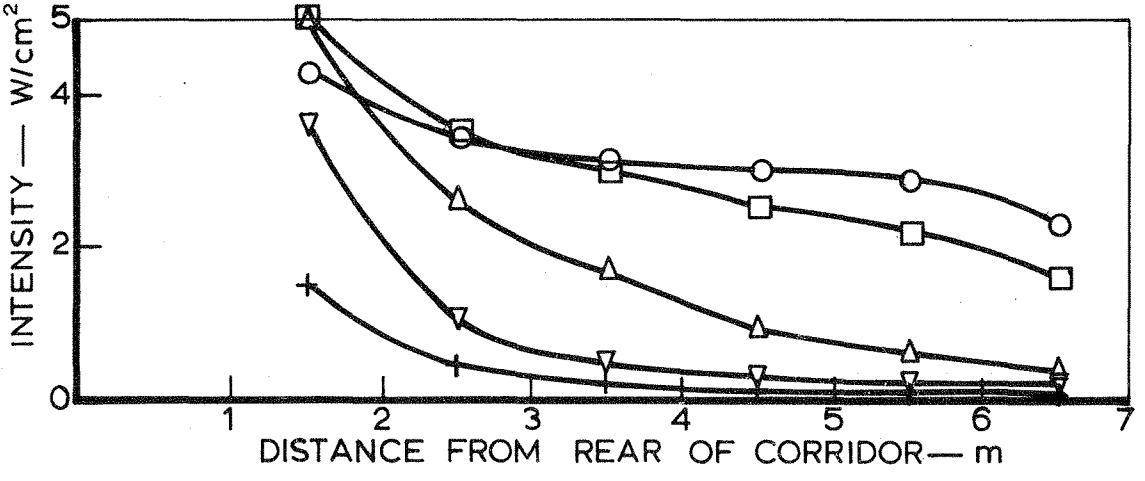

(b) Burner 37 cm beneath ceiling

Symbol	Gas flow per cm width cm³/s
○	300
□	250
△	183
▽	125
+	83

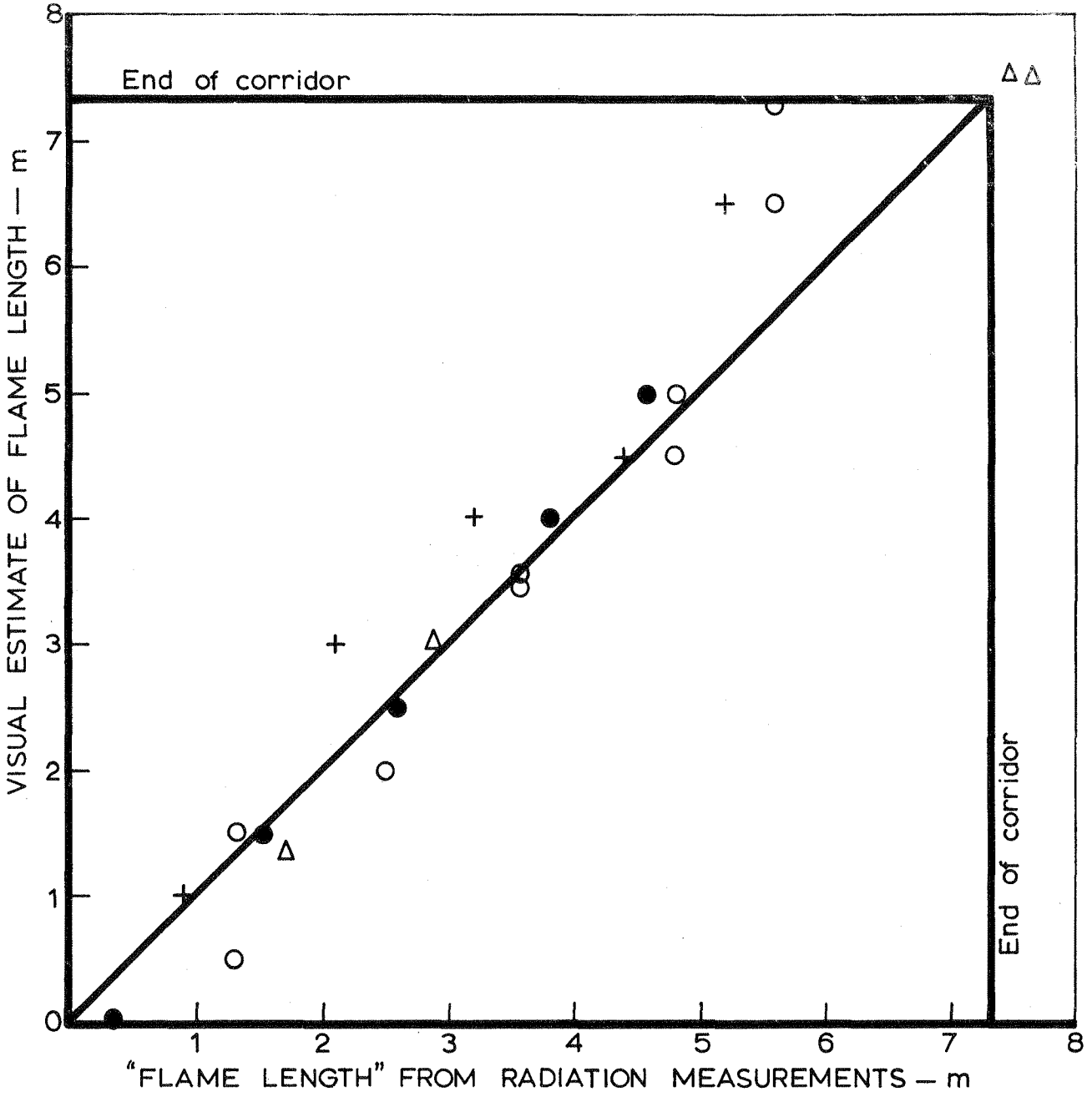

Symbol	Distance of burner beneath ceiling cm
Δ	37
O	66
+	90
●	120

Line is of 1:1 correspondence
Length measured from rear of corridor

FIG. 16. FLAME LENGTHS ESTIMATED VISUALLY COMPARED WITH THOSE ESTIMATED FROM RADIATION

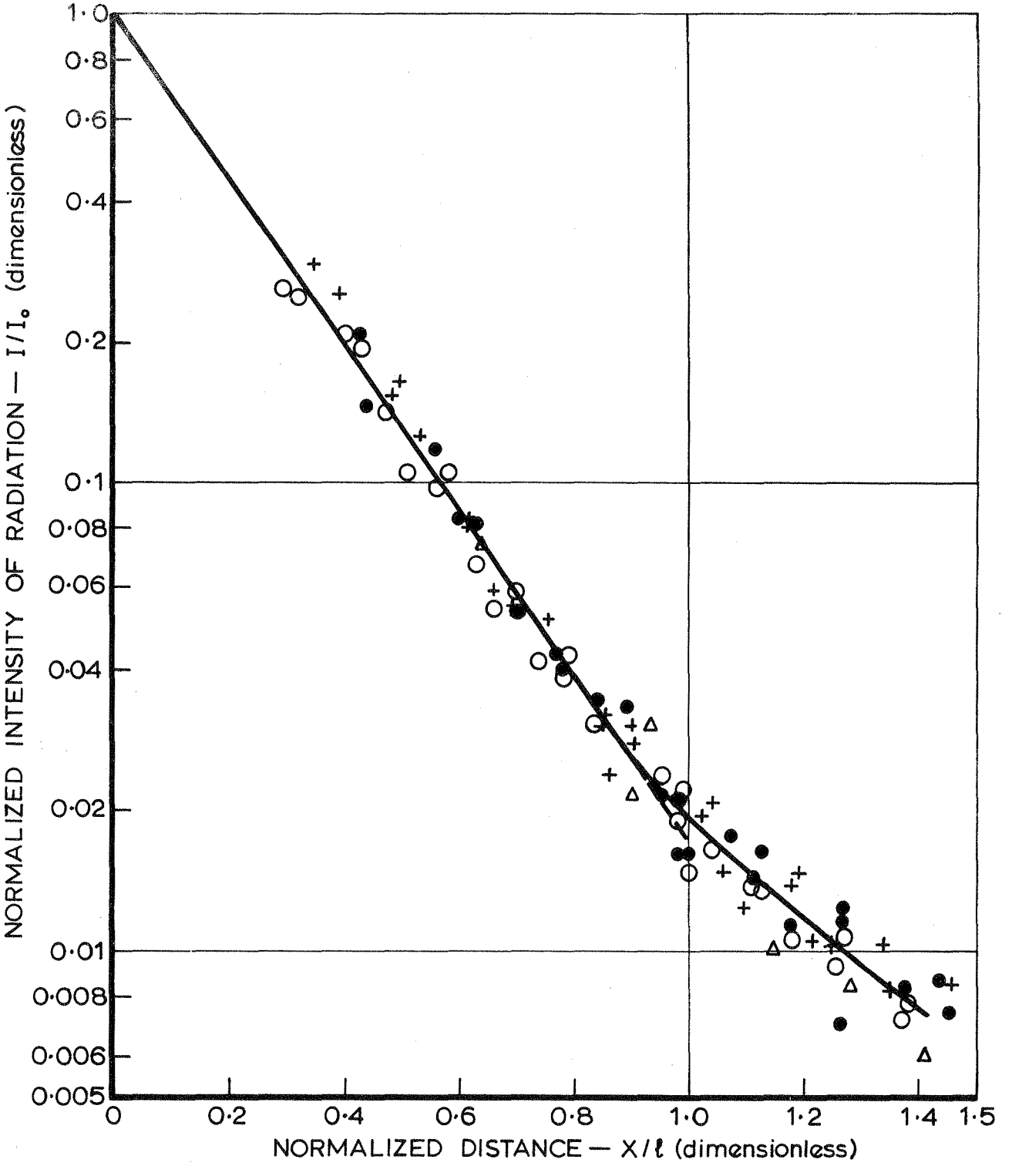

Symbol	Distance of burner beneath ceiling cm
△	37
○	66
+	90
●	120

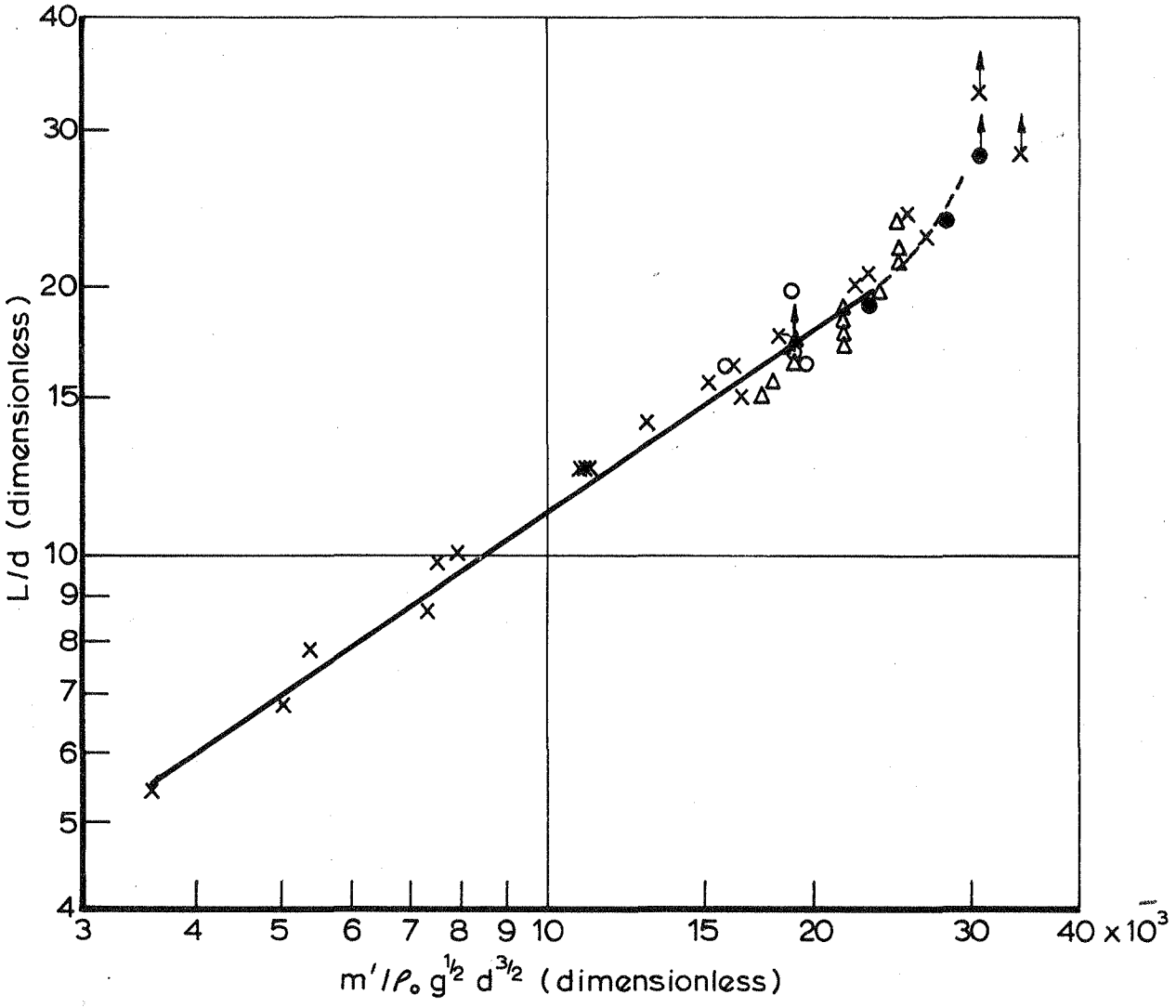

Depth of front end screen cm	Corridor length m	Symbol
0	7·3	×
0	5·8	●
15	5·8	△
23	5·8	○

Range of d — 18-60 cm

↑ — Indicates flames over end of corridor

FIG. 18. CORRELATION FOR HORIZONTAL FLAME LENGTHS

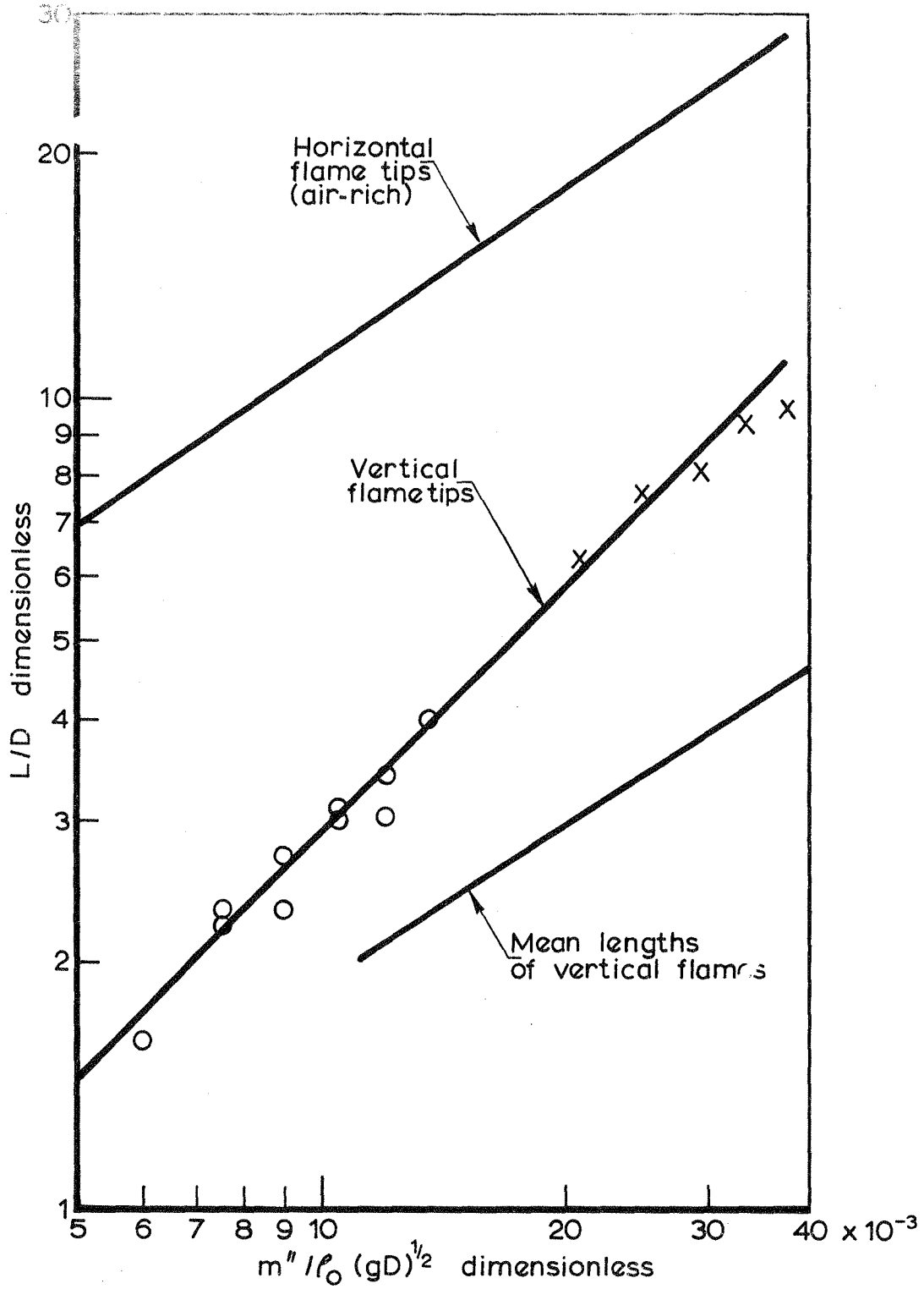

Symbol	Burner size m
O	1·2 x 0·3
X	1·2 x 0·15

FIG. 19. CORRELATION FOR FLAME LENGTHS

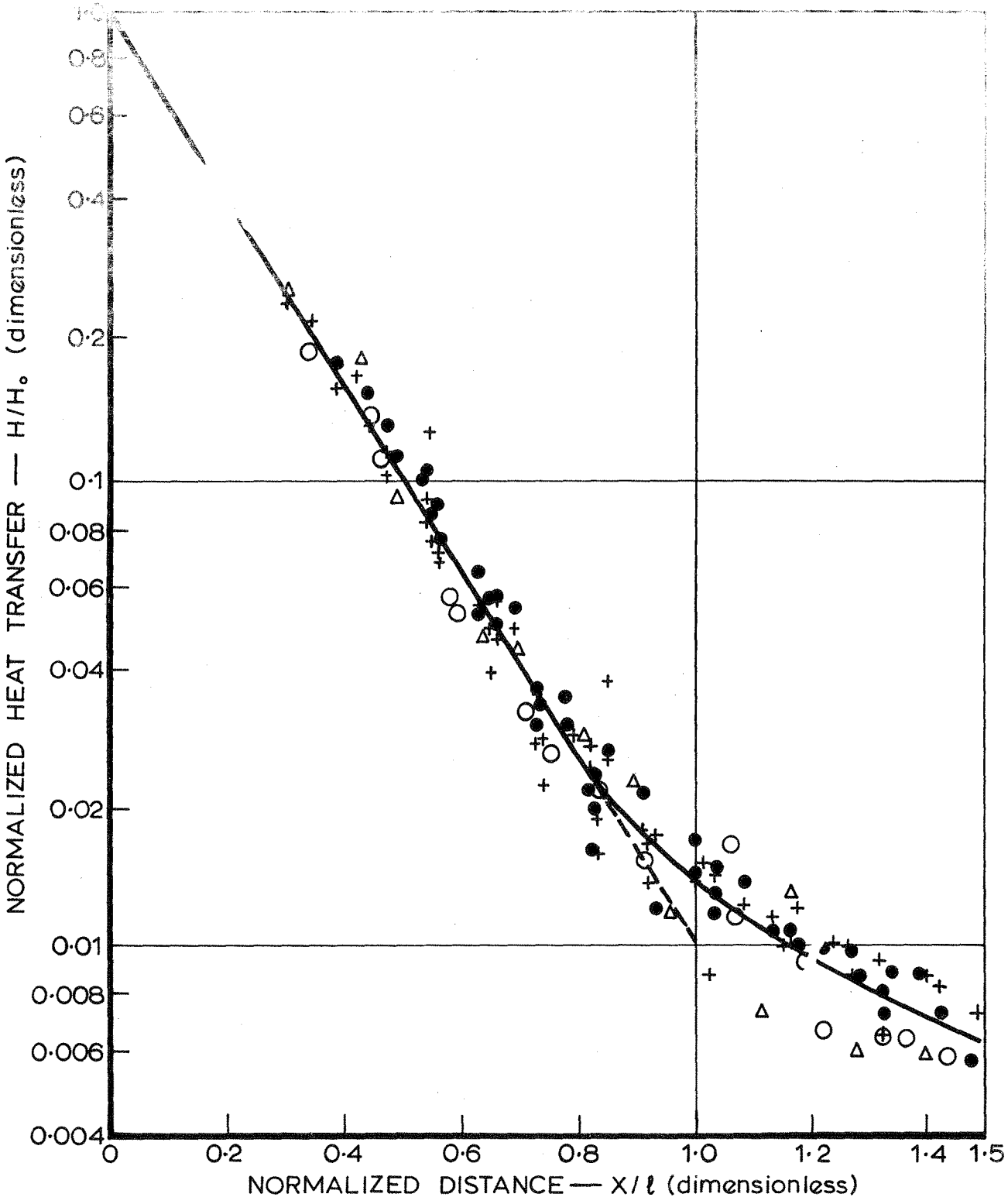

Symbol	Distance of burner beneath ceiling cm
Δ	37
O	66
+	90
●	120

1/6392 FR 712-

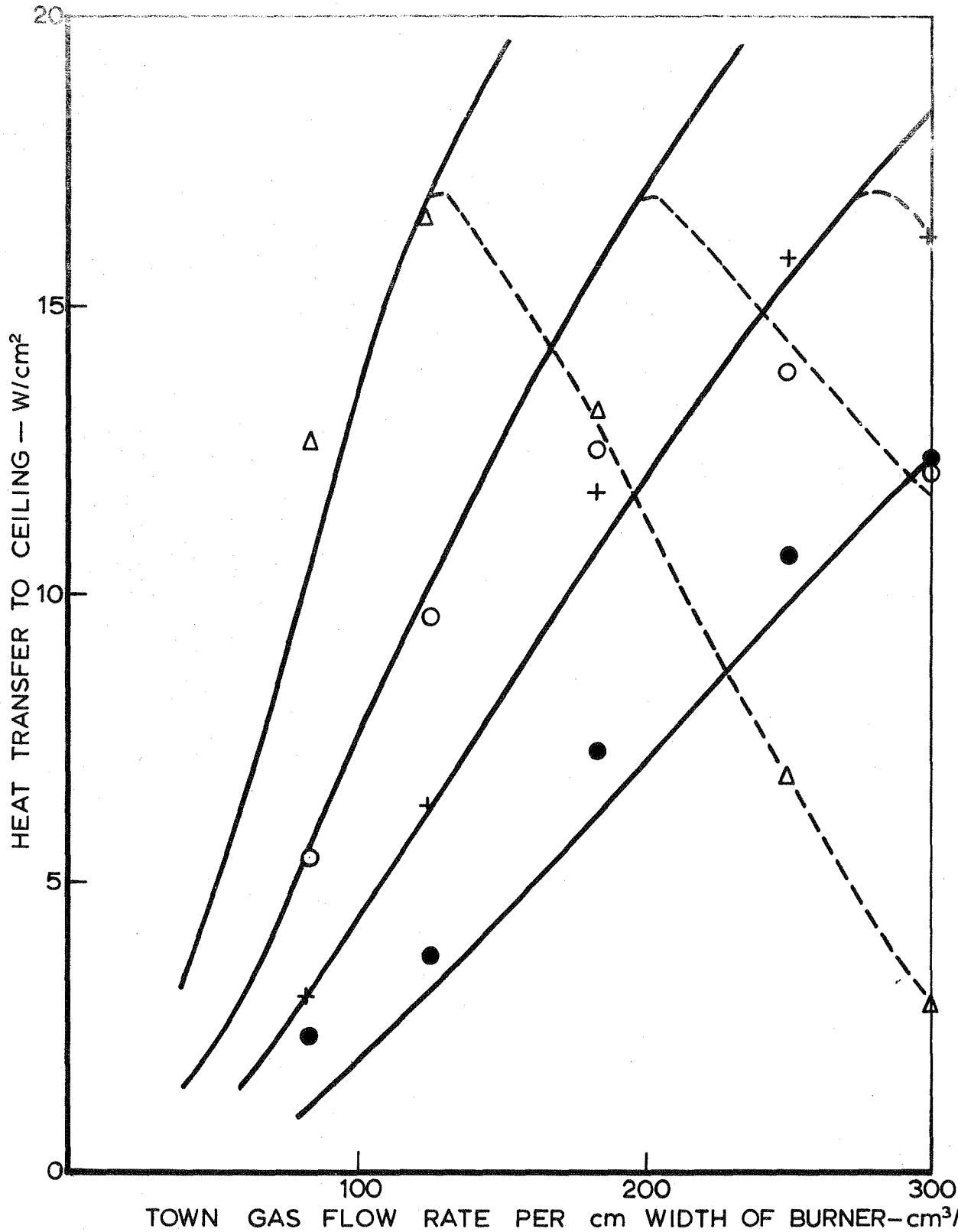

Symbol	Distance of burner beneath ceiling cm
Δ	37
O	66
+	90
●	120

Solid lines are equation $H = 70 \exp\left[-k \frac{x_o + 0.2}{0.152 V^{2/3}}\right]$

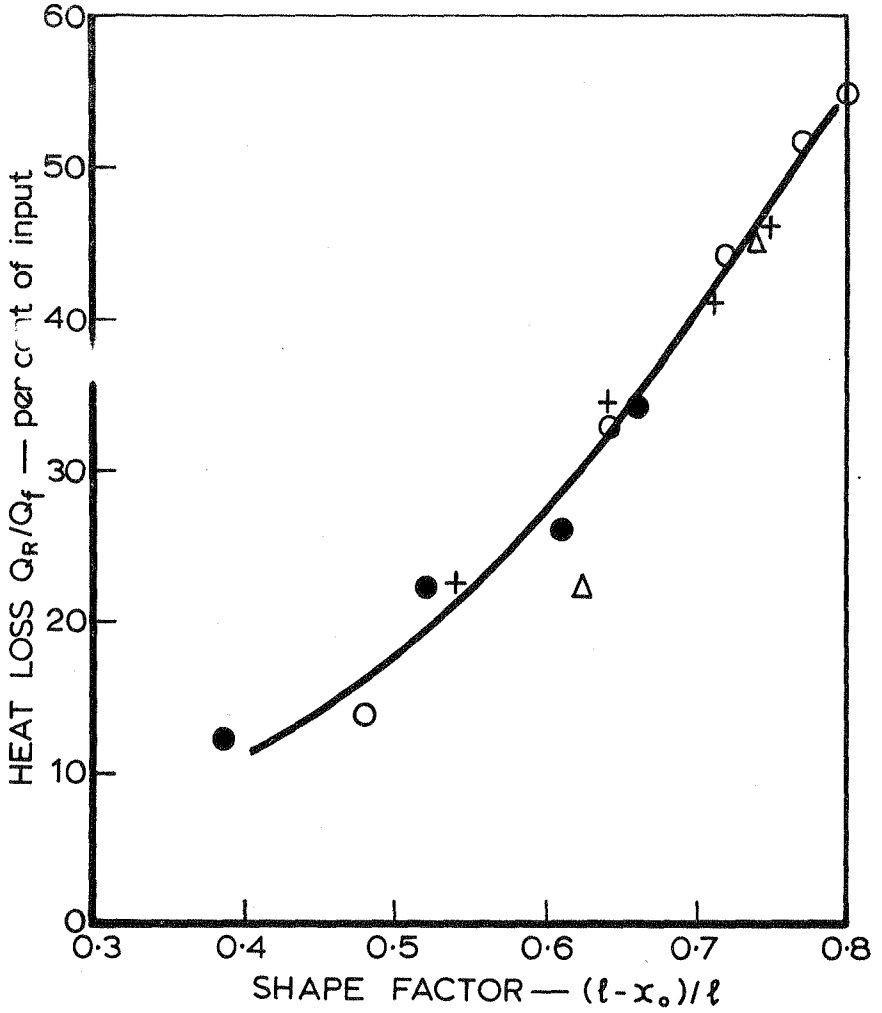

(a) By radiation

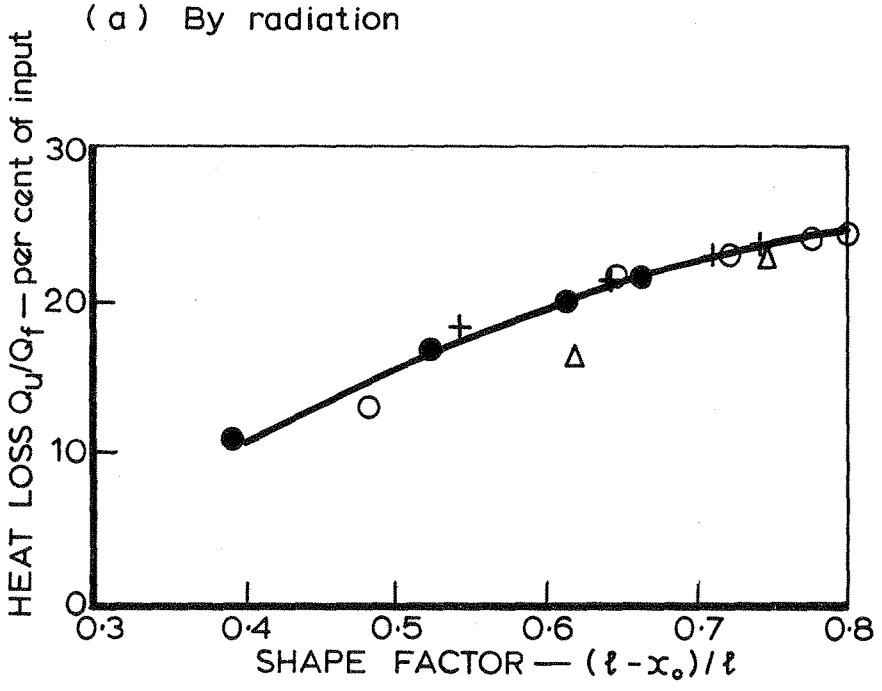

(b) Through ceiling and screens

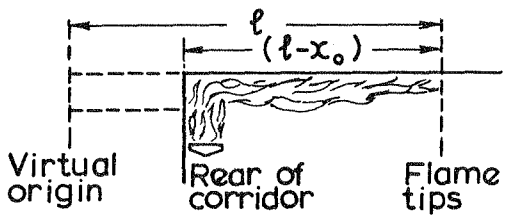

Symbol	Distance of burner beneath ceiling cm
Δ	37
O	66
+	90
●	120

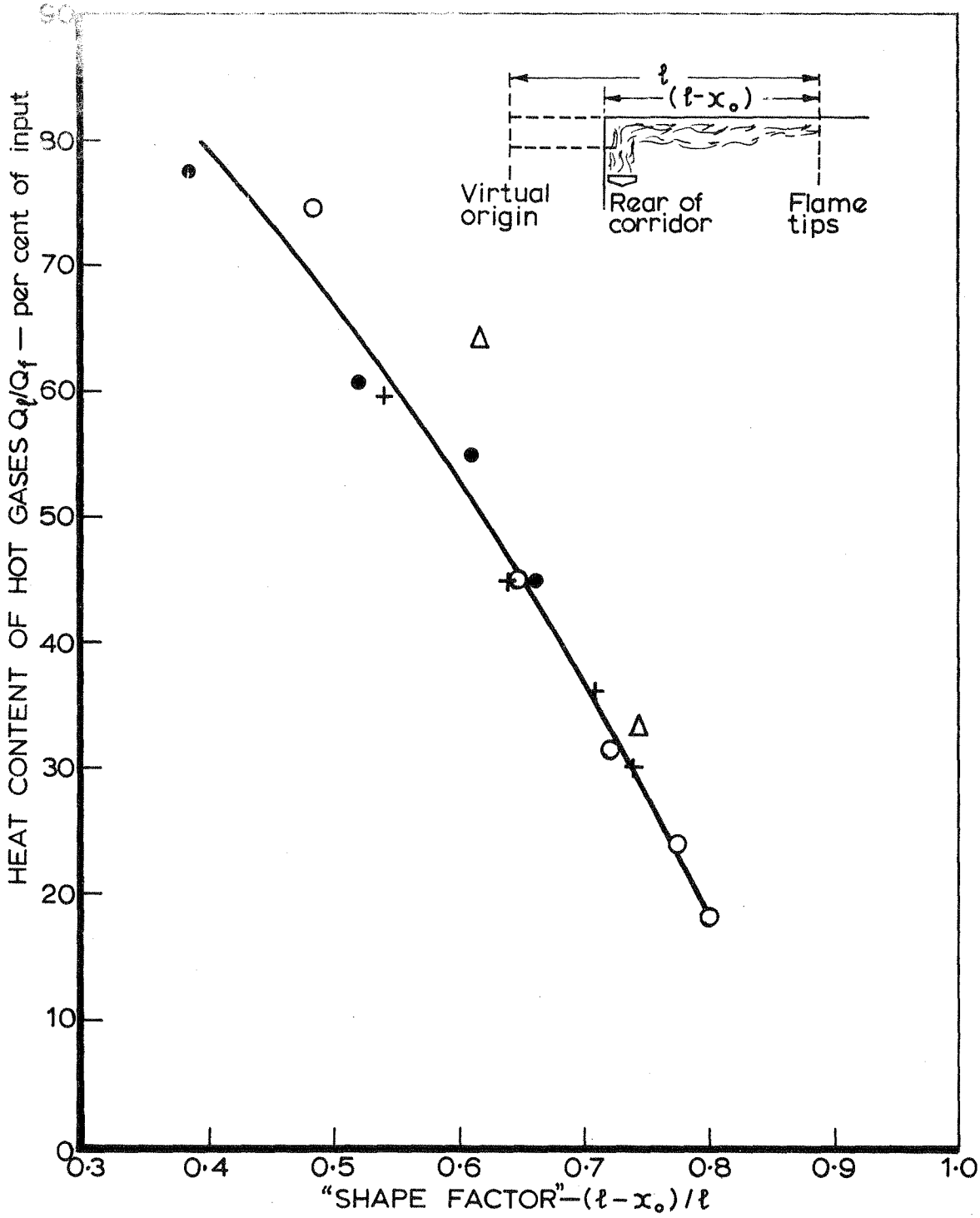

Symbol	Distance of burner beneath ceiling cm
Δ	37
O	66
+	90
●	120

F.R.712

11/8396

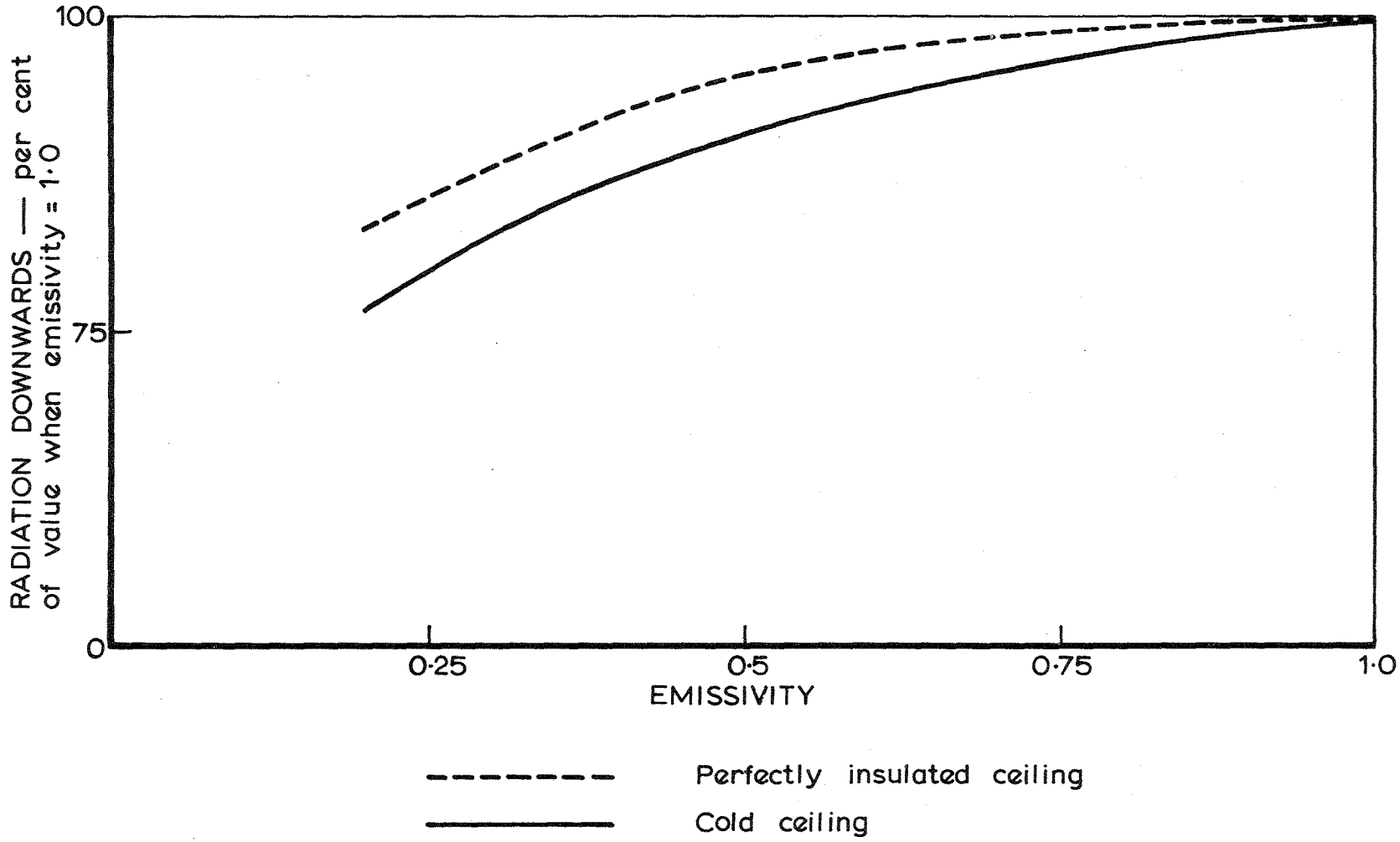

FIG. 24. EFFECT OF EMISSIVITY OF LAYER OF HOT GASES ON DOWNWARD RADIATION IN THE EXPERIMENTAL CORRIDOR

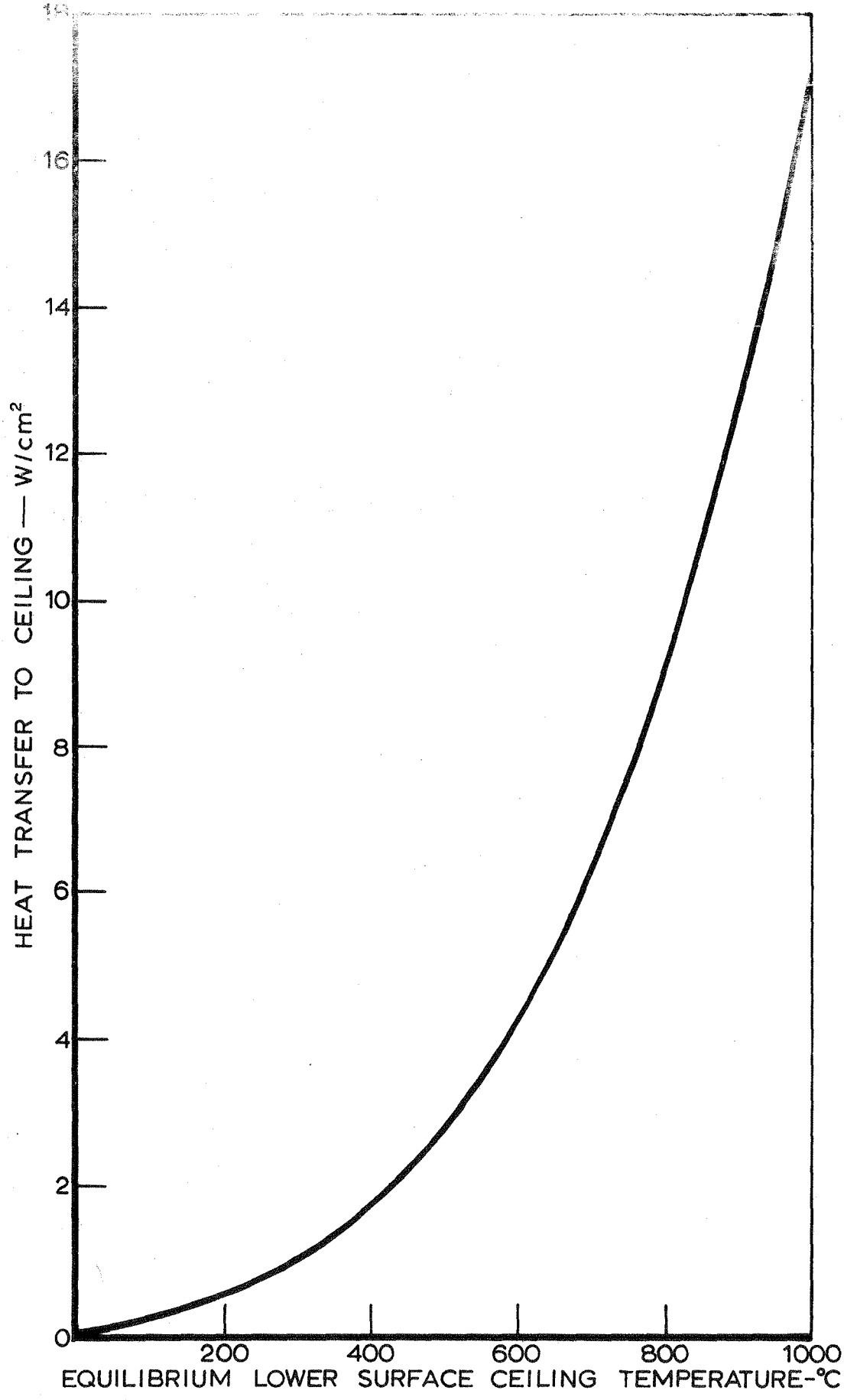
HEAT TRANSFER TO CEILING — W/cm²
0
2
4
6
8
10
12
14
16
200
400
600
800
1000
EQUILIBRIUM LOWER SURFACE CEILING TEMPERATURE-°C

1/8397 F.R. 712

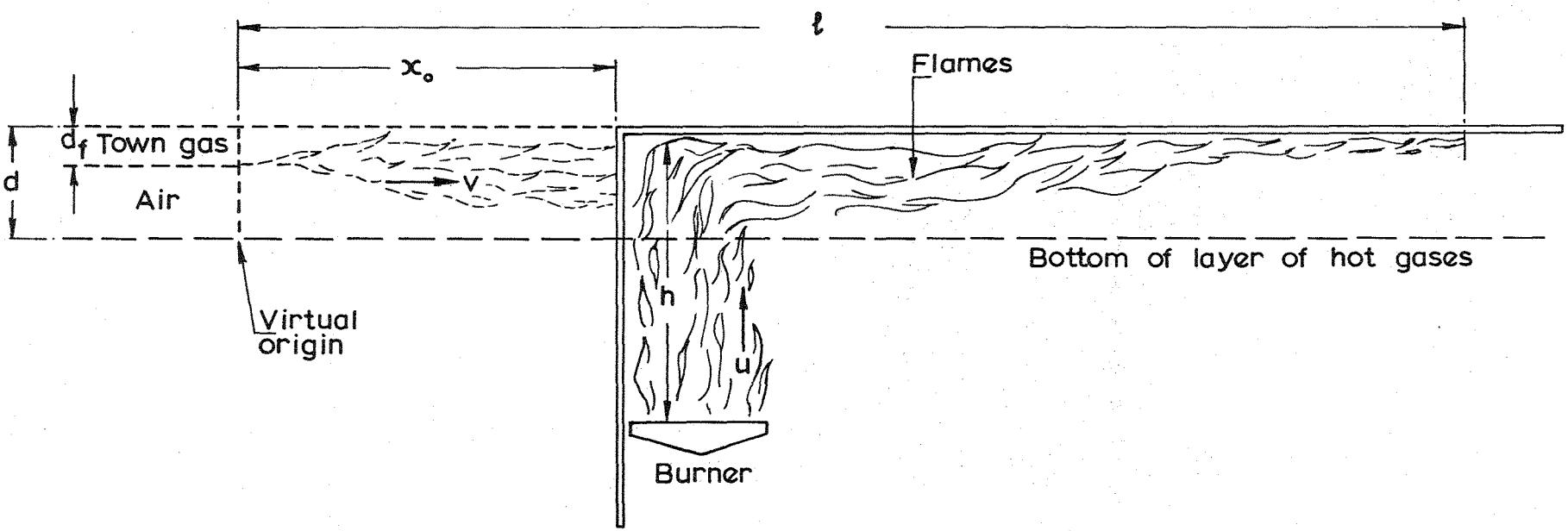

FIG. 26. VIRTUAL ORIGIN OF HORIZONTAL FLAMES

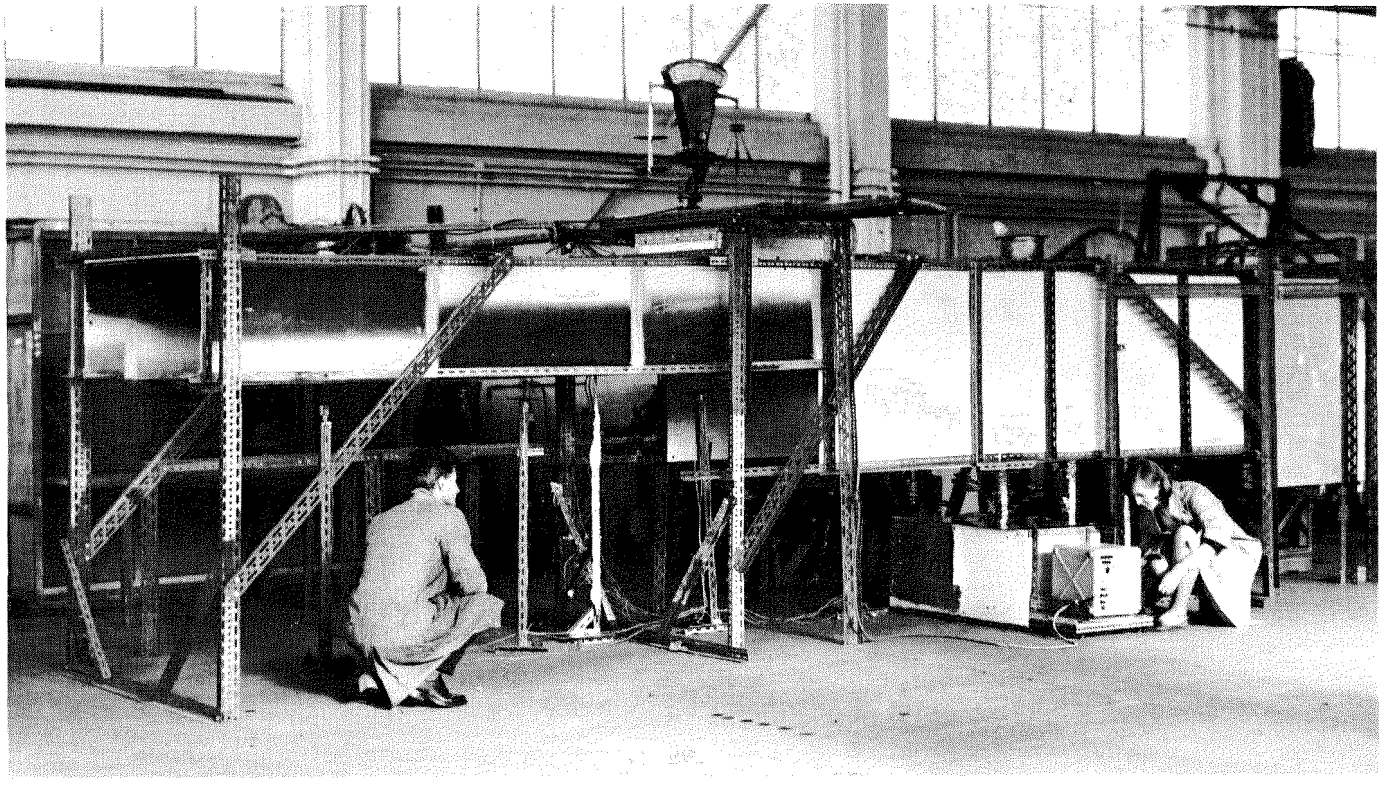

PLATE 1 GENERAL VIEW OF CORRIDOR

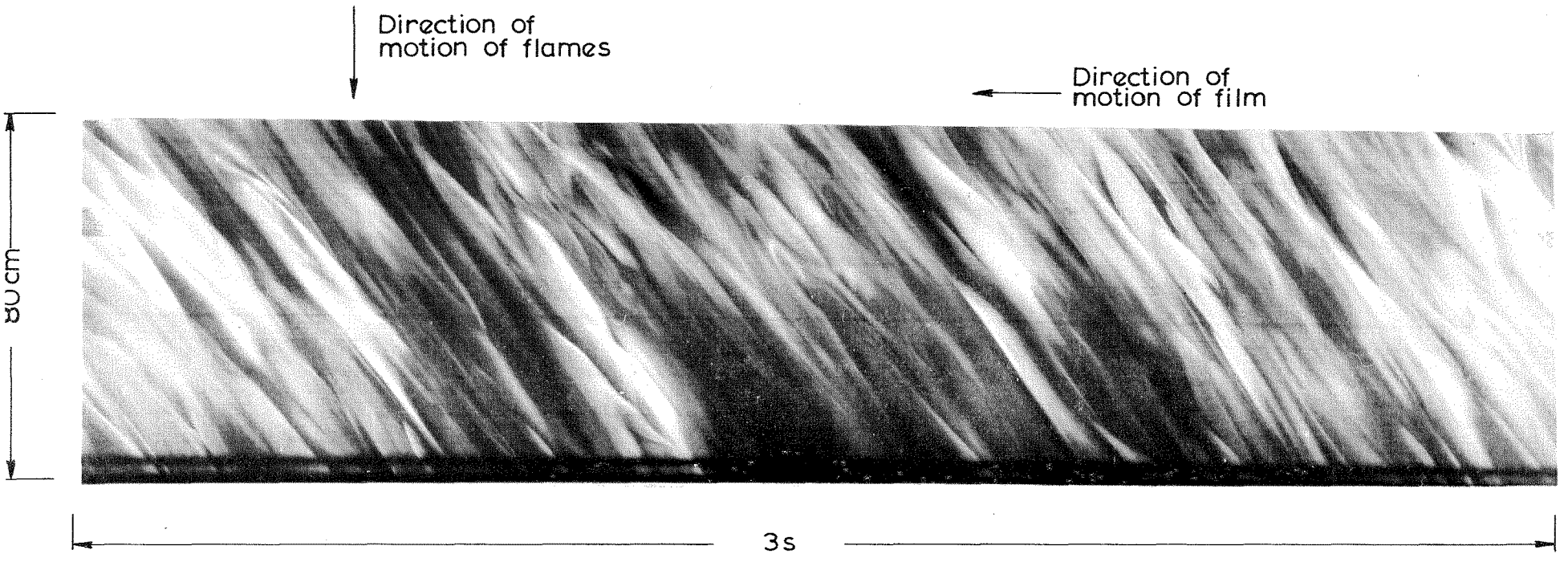

PLATE. 2. TYPICAL "STREAK" PHOTOGRAPH (POSITIVE PRINT)

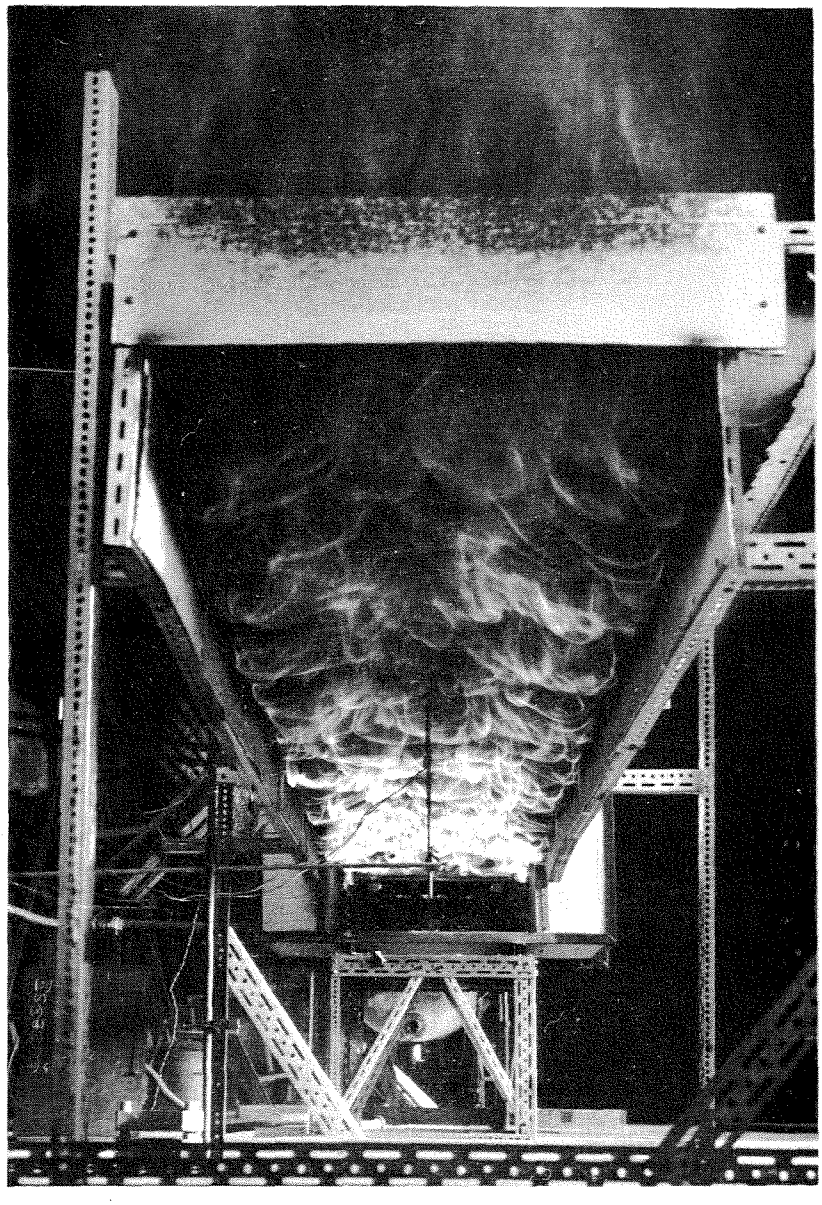

PLATE. 3. FLAMES BENEATH
CORRIDOR CEILING